Scube, a growth model for interior spruce in the SBS zone of British Columbia
Working document

Oscar García

July 19, 2010

Contents

1 Introduction

This is a draft working document written while proceeding with the project. As such, it includes some dead ends, and otherwise not-so-relevant material. It serves, however, as comprehensive and detailed documentation of results and procedures, more extensive than what would be possible to formally publish.

The approach borrows heavily from previous work, and I therefore ask for indulgence for what might seem as excessive self-citation.

2 Data

Data origin and selection criteria are briefly explained by Hu (2008). The data used for the mortality and basal area growth components consists of two distinct groups: (a) Young stands, less than 25 years-old (breast-height age), all planted except for one plot of natural origin (plot 5). (b) Older stands, older than 25 years, all of natural origin. Statistics are given in

	Mean	St.Dev.	Min.	Quartile 1	Median	Quartile 3	Max.
Site Index	19.7214	0.9729423	18.37178	18.67404	19.55129	20.50292	21.6468
B.H. Age (years)	11.89589	6.538499	1.64	6.7925	12.31	17.4175	23.45
Top Height (m)	5.403036	2.409044	1.66	3.5675	5.44	7.1725	10.27
Trees/ha	831.1554	439.4657	446.4	586.7	754.7	1026.075	3600
Basal Area (m^2/ha)	3.681304	3.832919	0.024	0.4685	2.177	6.41875	13.683
Initial N	862.7759	443.3027	471.9	612.2	766.0001	1088.4	3603.843
Site q	0.02005509	0.0007778207	0.0189742	0.0192171	0.0199202	0.02068045	0.0215922
Spruce %	99.5455	3.40114	74.5482	100	100	100	100

Table 1: Measurement statistics, young stands (breast-height age < 25, $n = 57$). All stands were planted (100% spruce), except for one of natural origin.

	Mean	St.Dev.	Min.	Quartile 1	Median	Quartile 3	Max.
Site Index	20.38382	1.842277	16.20505	19.02363	20.92554	21.69633	23.03833
B.H. Age (years)	51.88372	12.09975	27.5	44.5	52	59.5	76.5
Top Height (m)	20.64709	4.058714	10.75	18.22	20.79	23.0925	29.75
Trees/ha	1715.921	838.441	271.6	1111.1	1600	2133.925	5284
Basal Area (m^2/ha)	35.65113	8.349497	13.116	29.4685	36.933	41.15725	52.093
Initial N	2709.126	2177.891	286.09	1328.487	2364.134	3192.829	11615.62
Site q	0.02058142	0.001475013	0.0172191	0.0194976	0.0210175	0.02163165	0.0227003
Spruce %	81.17555	6.511963	71.6988	76.1836	78.3992	86.29715	95.3482

Table 2: Measurement statistics, older stands (breast-height age > 25, $n = 85$). All plots of natural origin.

	Mean	St.Dev.	Min.	Quartile 1	Median	Quartile 3	Max.
Site Index	20.12259	1.587708	16.20505	18.85356	20.32317	21.49363	23.03833
B.H. Age (years)	36.11387	22.12592	1.64	14.7325	39	54.5	76.5
Top Height (m)	14.63535	8.251686	1.66	6.3825	16.855	21.2375	29.75
Trees/ha	1366.999	829.1033	271.6	882	1087.4	1831.65	5284
Basal Area (m^2/ha)	23.04331	17.13478	0.024	4.1105	27.7345	38.25275	52.093
Initial N	1980.988	1938.047	286.09	907.0001	1145.106	2579.575	11615.62
Site q	0.02037385	0.001270512	0.0172191	0.0193612	0.020537	0.0214702	0.0227003
Spruce %	88.42004	10.54732	71.6988	78.1777	88.0476	100	100

Table 3: Measurement statistics, all ($n = 142$).

Tables 1–3. The last three rows in the tables are the estimated number of trees / ha at breast height, the site quality parameter q, and the percentage of interior spruce in the plots. See also Figures 1, 2, 3.

Not explained by Hu (2008): Natural PSPs have a threshold dbh below which trees are not measured in the main plot, mostly 2 cm (usually not a problem), but often 7.5 or 9.1 cm in the older measurements. Smaller trees are measured in a smaller sub-plot, or sometimes just counted. Basal areas and numbers of trees per hectare were calculated taking this into account as far as possible, using appropriate plot/subplot expansion factors, and sometimes a mean dbh for the excluded class.

In the natural plots, the most frequent secondary species was lodgepole

pine, in 52% of the measurements. Next was trembling aspen (22%), Engelmann spruce (10%), subalpine fir (9%), and poplar (5%). Douglas-fir and willow were recorded in one measurement each.

3 The model

The state of a stand at any time is described by four state variables: top height (H, metres), trees per hectare (N), basal area (B, m^2/ha), and relative cover (R). Relative cover is not directly observed, and represents the extent of the "resource capture apparatus" (foliage, fine roots), relative to that in a fully closed stand.

The growth model proper consists of one differential equation (DE) for each of the four state variables. In addition, there are some auxiliary relationships to predict outputs such as total and merchantable volumes, for the changes of state caused by thinning, site index calculations, etc.

The height and mortality sub-models for $\mathrm{d}H/\mathrm{d}t$ and $\mathrm{d}N/\mathrm{d}t$, respectively, are described in detail elsewhere, and only a brief summary is given below (t is time, in years). This report focuses on the development of the B and R components.

The DEs are integrated to predict the state at any time, given the state at some other time, provided that there are no disturbances (e.g., thinning) in between. The initial R is estimated indirectly. Implementation is simplified making use of "invariants" (or first integrals), quantities that remain unchanged in the absence of disturbances.

3.1 Height growth and site index

The growth rate equation is

$$\frac{\mathrm{d}H^c}{\mathrm{d}t} = b(a^c - H^c) \tag{1}$$

or, in the usual form of the Bertalanffy-Richards differential equation,

$$\frac{\mathrm{d}H}{\mathrm{d}t} = \frac{b}{c} H \left[\left(\frac{a}{H}\right)^c - 1 \right] ,$$

where H is stand top height (m) and t is time (years). The parameter $c = 0.5829$, $b = q$ is a parameter that varies among plots according to site quality, and $a = 283.87 q^{0.5137}$.

Integration of (1) gives the invariant

$$\ln[1 - (H/a)^c] + bt = \text{constant} , \tag{2}$$

that can be used to predict H_2 at time t_2, given a height H_1 at time t_1, by equating the corresponding invariants and solving for H_2:

$$H_2 = a\{1 - [1 - (H_1/a)^c]\mathrm{e}^{-b(t_2-t_1)}\}^{1/c} \,. \tag{3}$$

The site quality parameter q can be related to the traditional site index, defined as the predicted height at 50 years breast-height age, by substituting the breast-height and age-50 values in (3):

$$\text{Site Index} = a\{1 - [1 - (1.3/a)^c]\mathrm{e}^{-49.5b}\}^{1/c} \tag{4}$$

(defining breast-height age as number of rings at breast height, on average, breast height is reached at age 0.5). This equation needs to be solved numerically to calculate a value of q given a site index estimate.

Note that conventional site index curves correspond to substituting $H_1 = 1.3$ and $t_1 = 0.5$ in (3). This gives heights predicted "at birth". For growth projections, we use instead the current known height H_1 in (3). In particular, the predicted height at age 50 for an existing stand is in general different from the site index. For further discussion of these issues see García (2006).

3.1.1 Site scaling

For exploratory work, it is useful to transform variables in a way that makes relationships approximately independent of site quality. If a were a fixed constant in (1), with only $b \equiv q$ site-dependent, that could be achieved by scaling the observed ages proportionally to the estimated q (García, 1990; García and Ruiz, 2003).

Parameter values were $a = 38.19$ and $c = 0.5824$. In this instance, such a site-index model did not fit the data as well as the more complex one from the previous Section. Nevertheless, the estimated q was used to scale ages to the equivalent of site index 20 for graphical data analysis. The final mortality and basal area model did not depend on scaling.

Figure 1 shows the observed basal areas plotted over the scaled age. The scaling eliminates most of the variation due to site quality.

3.2 Mortality

The mortality model (or survival model, if you are an optimist), is fully described in García (2009). It uses a site-independent relationship for the mortality relative to height growth:

$$\frac{\mathrm{d}N}{\mathrm{d}H} = -aN^bH^c \,,$$

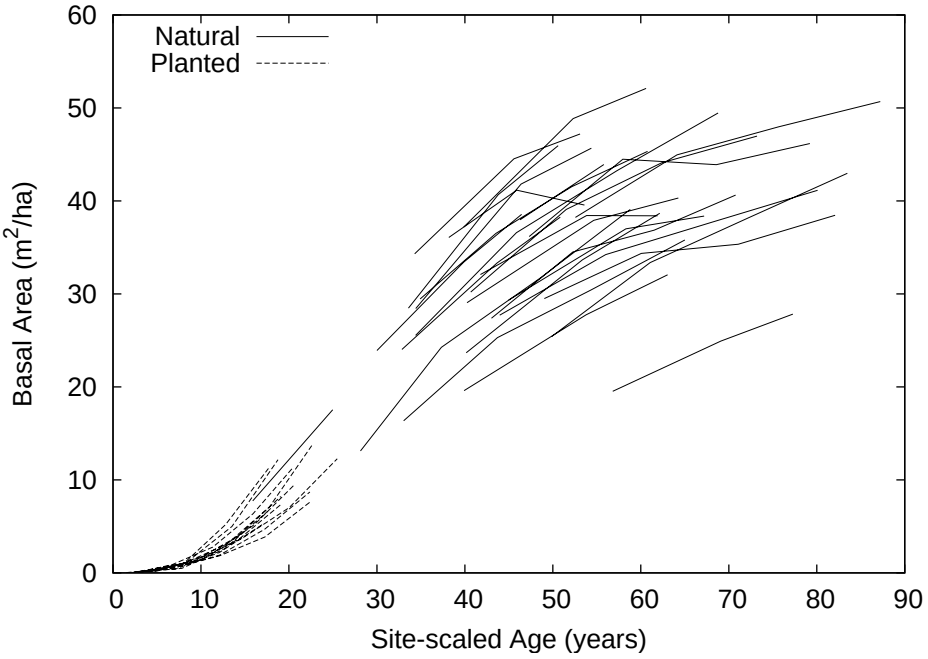

Figure 1: Sample-plot basal area over age scaled to site index 20 equivalent. Consecutive measurements on a same plot are joined by lines.

where a, b and c are constant parameters to be estimated (different from those in the previous section). An equation for $\mathrm{d}N/\mathrm{d}t$ could be obtained dividing by the one for $\mathrm{d}H/\mathrm{d}t$ above, but we will not need it.

The invariant, written in terms of the average spacing $S \equiv 100/\sqrt{N}$, is

$$S^{3.979} - (0.07213H)^{6.009} = \text{constant} \; . \tag{5}$$

A variation that includes species composition was also tried (Appendix A). Although it might be desirable for consistency when dealing with mixed-species stands, there was no improvement in predictions, and it was not used in the final model.

3.3 Basal area, closure

3.3.1 Gross increment

It is useful to model the growth of the product of basal area and height, $BH \equiv W$. This is approximately linearly related to total volume or biomass

per hectare. Unlike basal area (Figure 1), as a first approximation the gross volume or biomass increment is known to be roughly constant, for a closed-canopy stand in a given site (e.g., Assmann, 1970; García, 1990).

One can write

$$\frac{\mathrm{d}W}{\mathrm{d}t} = \text{gross increment} - \text{mortality} \; . \tag{6}$$

Here *gross increment* and *mortality* are in units of W per year. Following García and Ruiz (2003), this mortality can be expressed as the product of the mortality in number of trees, the average tree size, and a factor k smaller than 1, because dead trees tend to be smaller than average:

$$\text{mortality} = -k\frac{W}{N}\frac{\mathrm{d}N}{\mathrm{d}t} \; .$$

Values of k were estimated for each measurement interval by dividing the mean W of dead trees by the average W of live trees at both ends of the interval. The values were highly variable, but there were no clear trends with any stand variables. I will assume it constant, estimated by the average weighted by number of dead trees, 0.299, rounded to $k = 0.3$. Small differences will not significantly alter results.

Taking the mortality term to the left-hand side of (6),

$$\frac{\mathrm{d}W}{\mathrm{d}t} - k\frac{W}{N}\frac{\mathrm{d}N}{\mathrm{d}t} = \text{gross increment} \; ,$$

which can be written as

$$\frac{\mathrm{d}WN^{-k}}{\mathrm{d}t} = N^{-k} \times \text{ gross increment} \; . \tag{7}$$

This is easily verified by expanding the derivative of the product on the left-hand side of (7).

3.3.2 Closed stands

As already mentioned, in a closed-canopy stand fully utilizing the site potential, the gross W-increment on the right-hand side of (7) can be expected to change only slightly with stand conditions. It can be modelled as some function of N and/or H. I do not include B as a driving variable, because there are no plausible physiological mechanisms by which tree stem diameter would directly and significantly affect tree growth (García, 2009).

Figure 2 shows the changes in $WN^{-k} = BHN^{-0.3}$ over time. Once canopy closes, there are no indications of important changes in the slope

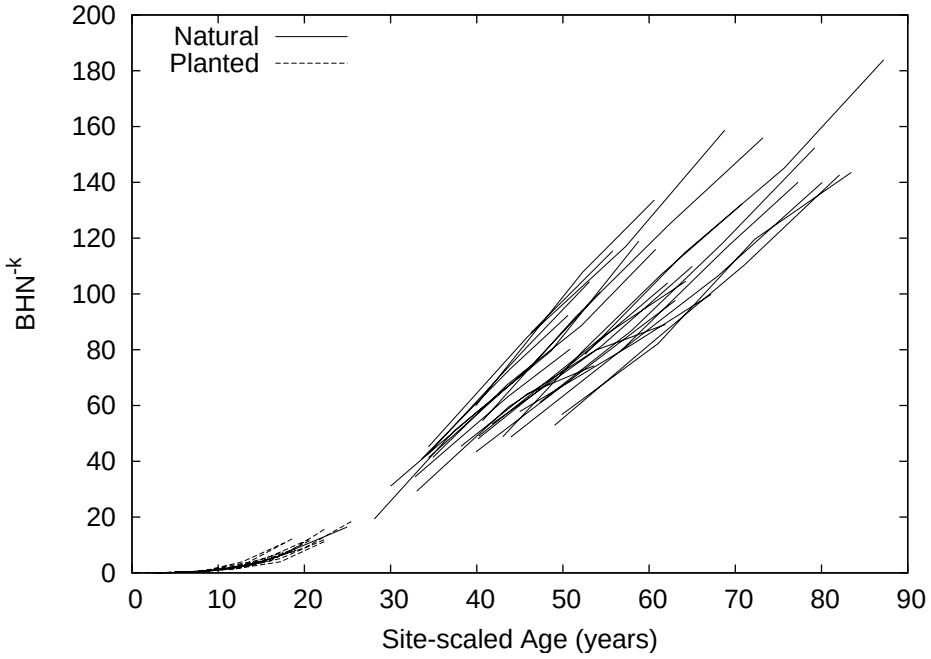

Figure 2: Observed trajectories from equation (7) . Ages scaled to site-index 20 equivalent.

given by equation (7). To analyze this further, the derivative in (7) was approximated by divided differences for each pair of consecutive measurements, and regressed over the mid-point values of N and/or H. Only measurements with $W > 200$ were used, to avoid instances where the site potential is not fully occupied. No significant regressions were found, with the best estimate being $\mathrm{d}WN^{-k}/\mathrm{d}t = 2.75$.

This would imply a W gross increment approximately proportional to $N^{0.3}$. García (1990) and García and Ruiz (2003) also found N to be the best predictor, with the increment increasing with N. A model based on this gave good results over the range of our data. However, extrapolating produced some trends of basal area over age with a seemingly unnatural upward curvature beyond about 100 years of (scaled) age. Although this might be considered a purely cosmetic issue, I sought an alternative that would produce plausible limiting behaviour.

The upward curving can be avoided by modelling the increment relative

to height increment as a function of height,

$$\frac{\mathrm{d}WN^{-k}}{\mathrm{d}H} = f(H)\ , \tag{8}$$

such that W does not keep increasing as H tends to its asymptote a. This also eliminates the need for age site-scaling, if Eichhorn's assumption about relationships between stand state variables being approximately independent of site quality is acceptable (Eichhorn, 1904; Assmann, 1970; Beekhuis, 1966; Mitchell and Cameron, 1985; García, 2009). It is seen in Figure 3 that the slopes increase with H.

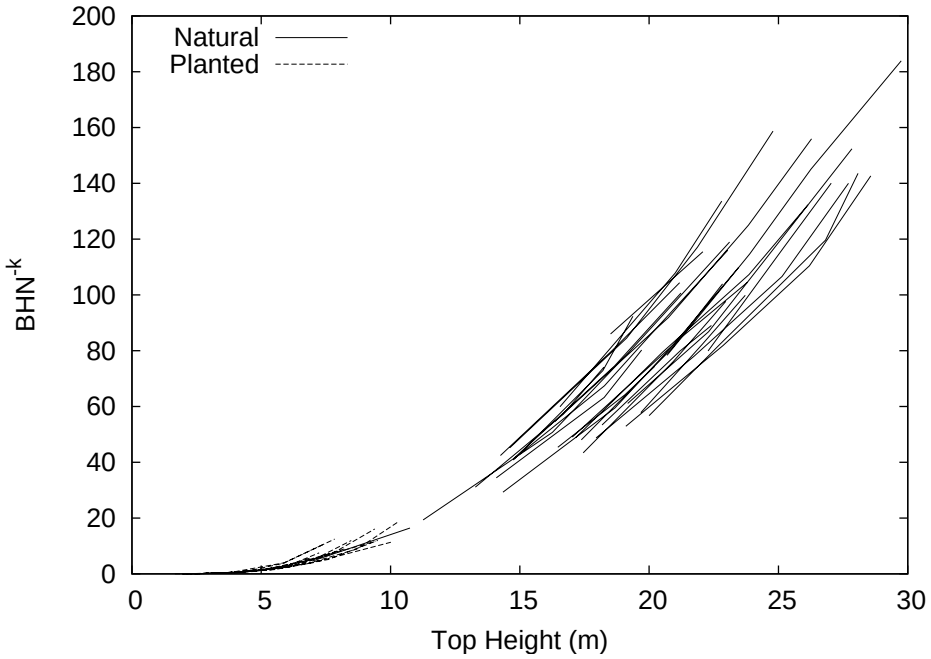

Figure 3: Observed trajectories from equation (8).

Again using finite difference approximations and $W > 200$, regressions for (8) showed no significant contribution from N, with the best functions being of the form

$$f(H) = \alpha(H + \beta)$$

or

$$f(H) = \alpha H^{1-\beta}\ ,$$

with essentially identical residual sums of squares. Least-squares parameter estimates for the linear function were $\alpha = 0.417$, $\beta = 3.48$, and for the power function $\alpha = 0.830$, $\beta = 0.180$ using logarithmic transformation, or $\alpha = 0.728$, $\beta = 0.132$, without it. There is considerable uncertainty in these estimates, though. Both function forms were tried in the complete model, re-estimating the parameters using the regression values as starting points.

Closed-canopy data is available only from natural stands. In the sample these may contain as little as 70% of spruce by basal area, with an average of 81%. Plantations can be expected to have a higher spruce content, and therefore higher spruce growth rates. Another difference is the use of genetically improved seed. Genetic improvement is often modelled simply through differences in site index (e.g., Buford and Burkhart, 1987), but the increases in basal area growth can be different from those in height (Carson *et al.*, 1999). It will be assumed that (8) differs between natural and planted by some factor, to be estimated later, expressed in different values of α in (9) or (10).

Update — Reexamination of the increment data showed the proportion of spruce as a significant predictor, either using observed values for each measurement, or plot averages. There were no obvious composition trends, and it was decided to use a plot average, calculated dividing the sum of the spruce basal areas from all the plot measurements by the sum of the all-species basal area. The best predictor was $f(H) = 0.60pH$, where p is the proportion of spruce. For more flexibility, I will use

$$f(H) = \alpha p(H + \beta) \tag{9}$$

or

$$f(H) = \alpha p H^{1-\beta} \,, \tag{10}$$

testing the significance of β later. Initial estimates are $\alpha = 0.6$, and $\beta = 0$.

3.3.3 Open stands

Young stands, or stands that have been recently thinned, do not yet have enough foliage and roots to capture all the available site resources. Their growth rate will be a fraction Ω of that in a fully closed stand. That is, (8) changes to

$$\frac{\mathrm{d}WN^{-k}}{\mathrm{d}H} = \Omega f(H) \,, \tag{11}$$

where the "relative occupancy" Ω is 1 for fully closed stands. Therefore, (8) becomes a special case of (11).

In open stands Ω increases as the amount of foliage and fine roots build up until reaching some dynamic equilibrium where $\Omega = 1$. Let R, called *relative closure*, represent the extent of this "assimilation apparatus" as a proportion of the maximum. It may be useful to think of R as amount of foliage (e.g., leaf area index), and of Ω as light interception, although these variables may also represent below-ground processes, and we do not need to be precise about the exact mechanisms.

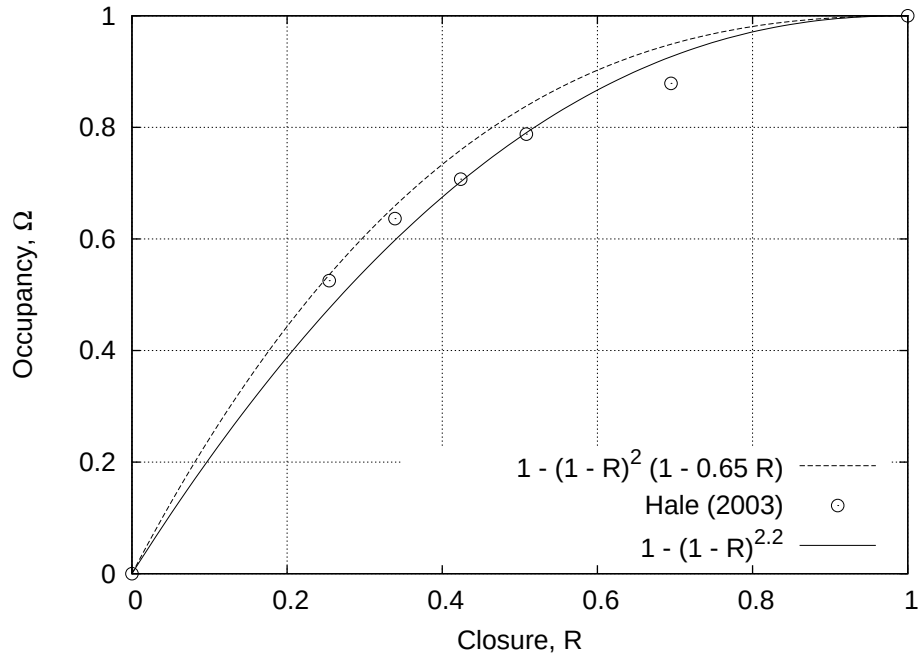

Figure 4: Relationships between relative occupancy and relative closure. Dashed curve inferred from radiata pine growth (García, 1989, 1990). Data points are measurements of relative light interception over thinning residual basal area in Sitka spruce (Hale, 2003). The continuous curve is used here.

Ω and R are non-linearly related. At low levels, resource capture increases in proportion to the assimilating material, but near the maximum an increase in R has a negligible effect on Ω. Leaves at the base of the canopy make a small or even negative contribution to net photosynthesis, and it is well-known that light thinning has a negligible effect on growth per hectare. The only attempt at determining such a relationship directly at

the stand level seems to be the work of Hale (2003), where light interception was measured after removing successively increasing proportions from a Sitka spruce stand in Scotland. Figure 4 compares a curve inferred from modelling the development of intensively managed radiata pine plantations (García, 1989, 1990), the measurements from Hale (2003), and the model

$$\Omega = 1 - (1 - R)^{2.2} \tag{12}$$

to be used here. It will be seen that the exact relationship is not critical.

It remains to model the growth of R (or of Ω) in less than fully-closed stands. It makes sense to assume that initially the increment of R relative to height increment is similar to that of W in (8), declining to 0 as full closure $R = 1$ is approached and the canopy base starts to lift:

$$\frac{\mathrm{d}R}{\mathrm{d}H} = g_1(R)\Omega f(H) \ ,$$

or, equivalently,

$$\frac{\mathrm{d}\Omega}{\mathrm{d}H} = g_2(\Omega)\Omega f(H) \ , \tag{13}$$

where g_1 and g_2 are decreasing functions over $(0, 1)$, such that $g_1(1) = g_2(1) = 0$.

In this model neither R nor Ω are observed, they are assumed to equal 1 in closed stands, or they are otherwise projected with the equations above, starting from suitable initial values. Before competition begins, R should be proportional to the number of trees. Therefore, we initialize R at breast height as

$$R_b = \min\{\rho N_b, 1\} \ , \tag{14}$$

where N_b is the number of trees per hectare at breast height, and ρ is a parameter to be estimated. On thinning, the current R is reduced in proportion to the basal area removed. R is converted to Ω with (12), and then projected with (13).

Given $g(\Omega)$, several strategies are possible for solving (11) and (13). Let

$$\int f(H)\,\mathrm{d}H \equiv x \ , \tag{15}$$

i.e., $x = \alpha p(H/2 + \beta)H$ for (9), or $x = \frac{\alpha p}{2-\beta}H^{2-\beta}$ for (10). Write also $g_2(\Omega)\Omega \equiv g(\Omega)$. Then, (13) is

$$\frac{\mathrm{d}\Omega}{\mathrm{d}x} = g(\Omega) \ , \tag{16}$$

a separable DE that gives

$$\int \frac{\mathrm{d}\Omega}{g(\Omega)} - x = \text{constant} \ ,$$

or

$$F^{-1}(\Omega) - x = \text{constant} \ , \tag{17}$$

where F describes the increase in occupancy, having the form of a growth function or cumulative probability distribution, with an upper asymptote of 1. That is,

$$\Omega = F(x + C) \ ,$$

with C being an integration constant. Substituting in (11),

$$\frac{\mathrm{d}WN^{-k}}{\mathrm{d}x} = F(x + C) \ ,$$

and

$$BHN^{-k} - \int F(x + C)\,\mathrm{d}x = \text{constant} \ .$$

Substituting $u = x + C$, the integral can be evaluated at $u = F^{-1}(\Omega)$:

$$BHN^{-k} - \int^{F^{-1}(\Omega)} F(u)\,\mathrm{d}u = \text{constant} \ . \tag{18}$$

An alternative is to write (11) as

$$\mathrm{d}WN^{-k} = \Omega\,\mathrm{d}x = \ \mathrm{d}x - (1 - \Omega)\,\mathrm{d}x$$

and eliminate the second $\mathrm{d}x$ with (16):

$$\mathrm{d}WN^{-k} = \ \mathrm{d}x - \frac{1 - \Omega}{g(\Omega)}\,\mathrm{d}\Omega \ .$$

Hence,

$$BHN^{-k} - x + \int \frac{1 - \Omega}{g(\Omega)}\,\mathrm{d}\Omega = \text{constant} \ . \tag{19}$$

The simpler approach of directly dividing (11) and (16) leads to difficulties with division by 0 as $\Omega \to 1$ (García, 1989).

3.3.4 Canopy closure models

From preliminary attempts at modelling early growth, it was thought that a model for (16) with two free parameters might be necessary. Such a model, that will be named "flexible", is described first. It was later found that a much simpler one-parameter model, "linear", gave similar results. A third one-parameter model, "logistic", was also tried.

Note that in the publication, the parameters θ and η used here were changed to $\gamma = 1/\eta$ and $\delta = \theta$.

A complex, flexible model It would be desirable to choose g so that the integrals can be calculated explicitly, avoiding the need for numerical integration. We want a closed-form growth function F, such that its integral can also be expressed in closed form (*cf.* (18)). We proceed backwards, first choosing an appropriate form for the integral $G(u) \equiv \int F(u)\,\mathrm{d}u$. Thereafter, $F(u) = \mathrm{d}G/\mathrm{d}u$ and, from (16) and (17),

$$g(\Omega) = \frac{\mathrm{d}\Omega}{\mathrm{d}x} = \left[\frac{\mathrm{d}x}{\mathrm{d}\Omega}\right]^{-1} = \left[\frac{\mathrm{d}F^{-1}(\Omega)}{\mathrm{d}\Omega}\right]^{-1} . \tag{20}$$

Without loss of generality, assume that u has been translated so that $F(0) = 0$, and choose $G(0) = 0$. It is seen that $u - G(u) = \int [1 - F(u)]\,\mathrm{d}u$, which is the accumulated loss from lack of occupancy, starts at 0 for $u = 0$ with a slope of 1. Then it increases with u, and the slope decreases monotonically toward 0, so that there is an upper asymptote. Therefore, $u - G(u)$ must take the shape of a "rounded ramp". A simple function with these properties, where the "rounding" can vary over a wide range depending on the shape parameter θ is

$$u - G(u) = \eta[1 + (u/\eta)^{-1/\theta}]^{-\theta} , \tag{21}$$

where η is the asymptote, and $0 < \theta \leq 1$ (Figure 5). This is the special case $ab = 1$ from the general two-shape-parameters family of curves in García (2008), with $b = -\theta$.

It follows from (21) that

$$F(u) = 1 - 1/[1 + (u/\eta)^{1/\theta}]^{\theta+1} , \tag{22}$$

and the invariant (17) for Ω becomes

$$\eta[(1 - \Omega)^{-1/(\theta+1)} - 1]^{\theta} - x = \text{constant} .$$

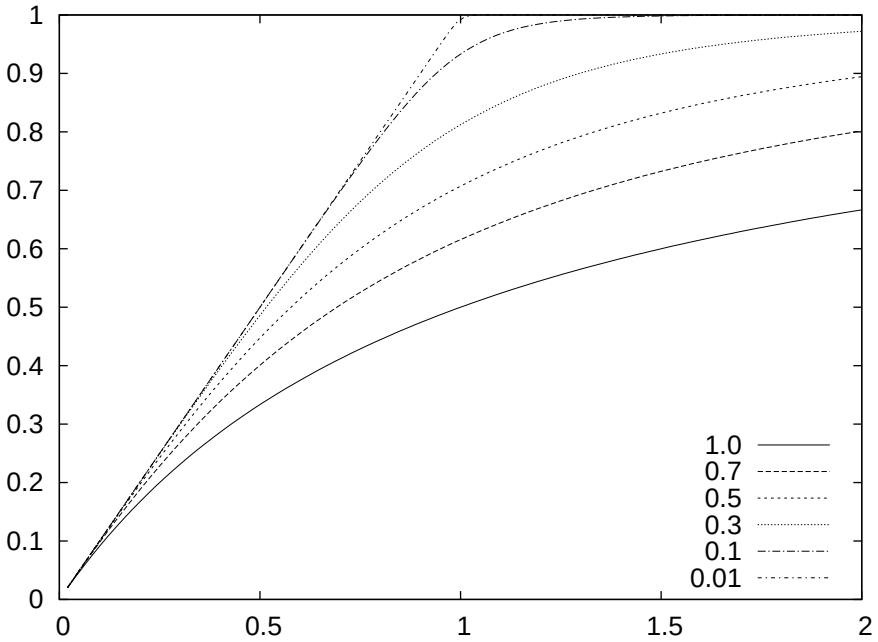

Figure 5: Rounded ramps from equation (21), for various values of θ. Axes in units of η.

The left-hand side becomes ∞ as $\Omega \to 1$, so it will be more convenient to use the reciprocal, written so as to avoid division by zero:

$$\frac{U^{\theta/(\theta+1)}}{\eta[1-U^{1/(\theta+1)}]^{\theta} - U^{\theta/(\theta+1)}x} = \text{constant} \ , \tag{23}$$

writing U for the "unoccupancy" $U = 1 - \Omega$.

Using (20) we obtain

$$g(\Omega) = \frac{\mathrm{d}\Omega}{\mathrm{d}x} = \frac{\theta+1}{\eta\theta} U^{1+\theta/(\theta+1)}[1-U^{1/(\theta+1)}]^{1-\theta} \ .$$

An equation for the closure growth rate $\mathrm{d}R/\mathrm{d}x$ or $\mathrm{d}R/\mathrm{d}H$ could be easily derived from this by using (12). Equation (22) is also a special case in García (2008), with $a = -1/(\theta+1)$ and $b = \theta$. As a check, it is found that the rate equation above agrees with the general formula given there.

Finally, the integral in the basal area invariant (19) turns out to be

$$\int \frac{1-\Omega}{g(\Omega)} \, \mathrm{d}\Omega = \eta[1-U^{1/(\theta+1)}]^{\theta} \ ,$$

so that the invariant is

$$BHN^{-k} - x + \eta[1 - (1 - \Omega)^{1/(\theta+1)}]^{\theta} = \text{constant} . \tag{24}$$

Linear The simplest possible model for (16) is a linear differential equation

$$\frac{\mathrm{d}\Omega}{\mathrm{d}x} = \tfrac{1}{\eta}(1 - \Omega) . \tag{25}$$

Separating variables,

$$\frac{\mathrm{d}\Omega}{1 - \Omega} = \tfrac{1}{\eta}\,\mathrm{d}x$$
$$-\,\mathrm{d}\ln(1 - \Omega) = \mathrm{d}\frac{x}{\eta} ,$$

giving an invariant

$$\ln(1 - \Omega) + x/\eta = \text{constant} ,$$

or, to avoid trouble when $\Omega \to 1$,

$$(1 - \Omega)\mathrm{e}^{x/\eta} = \text{constant} . \tag{26}$$

The basal area invariant (19) is

$$BHN^{-k} - x + \eta\Omega = \text{constant} . \tag{27}$$

Logistic Another simple model is the logistic differential equation

$$\frac{\mathrm{d}\Omega}{\mathrm{d}x} = \tfrac{1}{\eta}\Omega(1 - \Omega) . \tag{28}$$

Separating variables,

$$\frac{\mathrm{d}\Omega}{\Omega(1 - \Omega)} = \tfrac{1}{\eta}\,\mathrm{d}x$$
$$\mathrm{d}\ln\frac{\Omega}{1 - \Omega} = \mathrm{d}\frac{x}{\eta}$$
$$\ln(1/\Omega - 1) + x/\eta = \text{constant} ,$$

or

$$(1/\Omega - 1)\mathrm{e}^{x/\eta} = \text{constant} . \tag{29}$$

Equation (19) gives

$$BHN^{-k} - x + \eta\ln\Omega = \text{constant} . \tag{30}$$

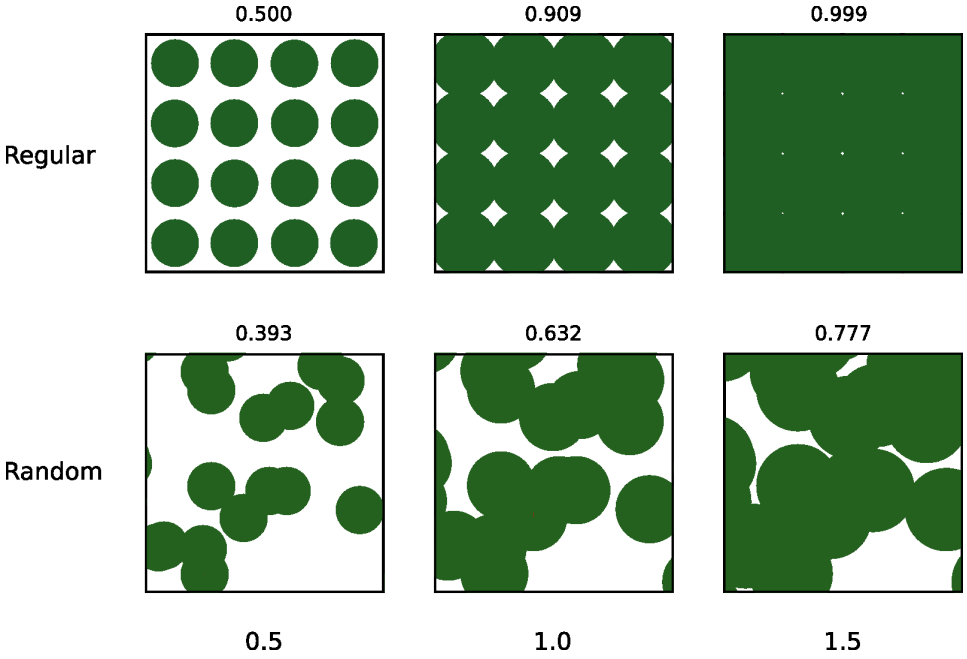

Figure 6: Illustration of the effect of spacing regularity on site occupancy. The circles represent a tree zone of influence (ZOI, Staebler (1951); Newnham (1964); Vanclay (1994)). Regular square spacing on the top row, and random (Poisson) locations on the bottom. The number of trees per unit area is the same. Columns correspond to total ZOIs per unit area of 0.5, 1.0, and 1.5. Numbers at the top of each diagram show the expected coverage area fractions. The ZOI might be expected to grow faster at higher occupancies, accentuating the differences for equal ages.

3.3.5 Natural *vs.* planted

Besides the difference in the growth rate αp of (9) or (10), natural and planted stands differ also in how fast they occupy the site in their early stages of development. As suggested by Figure 6, the irregular spacing of natural stands should be less efficient in this respect. For details, see Appendix B.

We model this by allowing a different scale parameter η in (21)–(24) for natural and planted stands.

3.4 Summary of projection equations

It is shown here how to project the state of a stand between two times t_1 and t_2, with no thinnings or other disturbances in-between. In case of thinning,

there is an instantaneous reduction in N and B, with the top height H assumed unchanged. R is reduced in proportion to the basal area removed. If either the residual B or N is not known, the relationships in García (2005) can be used to estimate one from the other for "typical" thinnings.

To make projections starting from bare-land, the stand state is initialized at breast-height age with $H = 1.3$, N assumed known, $B = 0$, and R from (14).

Suppose that at time t_1 the state of the stand is (H_1, N_1, B_1, R_1). In general, R_1 is not directly measured, but it can be estimated in one of several ways:

1. If the current state is the result of a model projection, R_1 is already available.

2. If the stand is considered to be fully closed, e.g., if the base of the canopy is rising, take $R_1 = 1$.

3. If the stand has just been thinned, the R before thinning, usually 1, is reduced in proportion to the basal area removed.

4. For a young open unthinned stand, estimate an initial R_b at breast-height age from (14), and project it to t_1 as shown below. In complicated cases with several thinnings it might be necessary to alternate projections and thinning reductions.

Projection can be done efficiently by computing the invariants at t_1, and then inverting them to recover the state at t_2. Some care is needed to avoid invalid arguments in intermediate operations. In detail, for the *flexible* closure model, compute the following invariant values, derived from (2), (5), (23), and (24):

$$
\begin{aligned}
y_1 &= \ln[1 - (H_1/a)^c] + bt_1 \\
y_2 &= (100/\sqrt{N_1})^{3.979} - (0.07213 H_1)^{6.009} \\
y_3 &= \frac{(1 - R_1)^{2.2\theta/(\theta+1)}}{\eta[1 - (1 - R_1)^{2.2/(\theta+1)}]^\theta - (1 - R_1)^{2.2\theta/(\theta+1)} x(H_1)} \\
y_4 &= B_1 H_1 N_1^{-k} - x(H_1) + \eta[1 - (1 - R_1)^{2.2/(\theta+1)}]^\theta
\end{aligned}
$$

Here, $x(H) = \alpha p(H/2 + \beta)H$ if using (9), or $x(H) = \frac{\alpha p}{2-\beta} H^{2-\beta}$ for (10). The y_i do not change between t_1 and t_2, so that the equations are valid with t_2 and the state at time t_2 substituted on the right-hand sides. The new state

is obtained by solving the y_i equations sequentially:

$$
\begin{aligned}
H_2 &= a[1-\exp(y_1 - bt_2)]^{1/c} \\
N_2 &= 10000/[y_2 + (0.07213H_2)^{6.009}]^{2/3.979} \\
R_2 &= 1 - \left\{ \frac{[\eta y_3/(y_3 x(H_2)+1)]^{1/\theta}}{[\eta y_3/(y_3 x(H_2)+1)]^{1/\theta}+1} \right\}^{(\theta+1)/2.2} \\
B_2 &= N_2^k \{ y_4 + x(H_2) - \eta[1-(1-R_2)^{2.2/(\theta+1)}]^\theta \}/H_2
\end{aligned}
$$

If $R_1 = 1$, the calculation of y_3 and R_2 can be omitted, because then $R_2 = 1$ (and the equations for y_4 and B_2 simplify).

Usually $t_2 > t_1$, but the procedure is also mathematically valid for projections back in time, that are occasionally useful. The back-projection of R, however, can be numerically unstable if R_1 is close to 1. In that situation, R_2 could be calculated first by projecting forward from breast height.

An implementation of these projections in the R computer language is given in Appendix C.

For the *linear* closure model we have instead,

$$
\begin{aligned}
y_3 &= (1-R_1)^{2.2} \exp[x(H_1)/\eta] \\
y_4 &= B_1 H_1 N_1^{-k} - x(H_1) + \eta[1-(1-R_1)^{2.2}] \\
R_2 &= 1 - \{ y_3 / \exp[x(H_2)/\eta]] \}^{1/2.2} \\
B_2 &= N_2^k \{ y_4 + x(H_2) - \eta[1-(1-R_2)^{2.2}] \}/H_2
\end{aligned}
$$

For the *logistic*:

$$
\begin{aligned}
y_3 &= \{ 1/[1-(1-R_1)^{2.2}] - 1 \} \exp[x(H_1)/\eta] \\
y_4 &= B_1 H_1 N_1^{-k} - x(H_1) + \eta \ln[1-(1-R_1)^{2.2}] \\
R_2 &= 1 - \{ 1 - 1/[1 + y_3 / \exp(x(H_2)/\eta)] \}^{1/2.2} \\
B_2 &= N_2^k \{ y_4 + x(H_2) - \eta \ln[1-(1-R_2)^{2.2}] \}/H_2
\end{aligned}
$$

4 Parameter estimation

4.1 Estimation criteria

Statistical parameter estimation usually proceeds by taking as given a deterministic or nominal model, and assuming some stochastic structure for the deviations. Then the parameter estimates are chosen so as to optimize a

criterion such as maximum likelihood or Bayesian posterior expectation. In this instance, a satisfactory error model might involve adding noise to the growth rates, to obtain stochastic differential equations (Seber and Wild, 2003). Any optimal properties and error estimates, however, are conditional on the nominal and stochastic models being "true". There is little guidance about the effects of model misspecification. Here I take a more heuristic and direct approach, trying to obtain a good over-all fit to the observations, while avoiding biases for particular growing conditions.

Estimation in dynamic models can be based on projections over a variety of time intervals (Bard, 1974; Borders *et al.*, 1988; Seber and Wild, 2003). I obtained parameter estimates by minimizing a root mean square error (RMSE) calculated in four different ways:

1. From breast height. Many applications require predictions starting from bare land. Model evaluation also typically looks at the quality of such predictions (Goulding, 1979; Vanclay and Skovsgaard, 1997). It seems natural therefore to minimize these deviations. In this case, projections for each measurement occasion were calculated starting from breast height, with basal area zero, and initial number of trees estimated with (5) using the first available measurement. The initial R is given by (14).

2. Shortest intervals. Observed sizes on a same plot are highly correlated, because they correspond to accumulated growth over overlapping time intervals. Deviations for projections starting from the first point in each pair of consecutive measurements are more nearly independent, leading to better statistical properties (Borders *et al.*, 1988; Seber and Wild, 2003). On the other hand, minimizing deviations over each of these steps ignores the possibility of accumulating bias over longer time spans if the model is poor. The RMSE included an estimate for the first measurements, starting from breast height as described above.

3. Weighted shortest. Although the deviations for non-overlapping intervals may be considered as statistically independent, their variances vary with the interval length. Under certain conditions, the variance increases roughly proportionally to time, and an RMSE with inverse weighting by interval time length follows statistical theory more closely (Seber and Wild, 2003). In this instance the effect is mainly a reduced contribution of the long intervals from breast height to first measurement. Perhaps not so good, given their impact on long-term predictions.

$f(H)$	Crit.	RMSE	α	β	θ	η_p	η_n	ρ
power	1	2.925	0.8992	0.1805	0.9214	29.90	17.99	1.801×10^{-30}
power	2	1.913	0.4107	-0.0894	0.7513	9.36	7.38	1.630×10^{-34}
power	3	1.213	0.7427	0.0939	0.7308	19.90	19.13	4.074×10^{-18}
power	4	1.587	0.7066	0.1033	0.8870	20.99	12.55	2.915×10^{-32}
linear	1	2.927	0.4600	2.4513	0.7378	24.80	15.31	9.613×10^{-30}
linear	2	1.914	0.5356	0.3282	0.8516	17.14	14.44	6.220×10^{-23}
linear	3	1.213	0.5240	1.2447	0.6289	19.39	18.67	5.210×10^{-18}
linear	4	1.587	0.4833	1.3413	0.7611	19.37	11.83	1.553×10^{-31}

Table 4: Parameter estimation results, different η for planted and natural. *Flexible* closure model.

4. Weighted from breast height. Finally, an RMSE was calculated with predictions as in point 1 and inverse time weighting as in 3. This might to some extent attenuate the redundancy from interval overlapping.

Special consideration was given to sample plot 23, the older plot that appears below the others toward the bottom-right of Figure 1. It starts at a rather low density of 284 trees per hectare. It might be that it had sparse regeneration, but it seems equally likely to have suffered a disturbance later in life. Therefore, projections were started from its first measurement, rather than from breast height.

4.2 Fitting results

The RMSE calculations were programmed in R (R Development Core Team, 2009), and the values minimized using the BCFGS method of function `optim` (Appendix C).

First results are given in Table 4, for the *flexible* closure model. Note that RMSE is not comparable across criteria, because it corresponds to different types of residuals. The power and linear forms of (8) gave very similar fits, and only the power form (10) will be used in what follows. The differences in *eta* between planted and natural are in the wrong direction. The inclusion of species composition may already account for the lower coverage efficiency of natural stands, which may result in the appearance of other species. Parameters were therefore re-estimated using a common *eta* (Table 5).

Convergence of the models of Tables 4 and 5 was often problematic, sometimes requiring several attempts with various starting points in order to obtain a solution. Especially so for criterion 1. In those instances, the optimization procedure failed to find a suitable gradient after repeatedly

Crit.	Interval	Weights	RMSE	α	β	θ	η	ρ
1	no	no	2.97826	0.877449	0.1733650	0.564232	15.3474	1.34192×10^{-12}
2	yes	no	1.91884	0.488115	-0.0341464	0.736746	10.6266	1.56572×10^{-6}
3	yes	yes	1.21346	0.713011	0.0810126	0.701253	18.4312	3.19829×10^{-6}
4	no	yes	1.63074	0.683038	0.0879667	0.579671	13.7252	5.52263×10^{-6}

Table 5: Parameter estimation results. Common η, $f(H) = \alpha p H^{1-\beta}$, *flexible* closure model.

Crit.	Interval	Weights	RMSE	α	β	η	ρ
1	no	no	2.994278	0.7473692	0.1175678	13.2128	1.586627×10^{-7}
2	yes	no	1.919436	0.4150594	-0.08552999	7.317568	1.823453×10^{-6}
3	yes	yes	1.216236	0.6027009	0.02953962	12.97816	1.619716×10^{-6}
4	no	yes	1.641956	0.6005521	0.04069049	11.44467	4.224663×10^{-6}

Table 6: Parameter estimation results. *Linear* closure model.

Crit.	Interval	Weights	RMSE	α	β	η	ρ
1	no	no	3.046414	0.4516738	-0.04398175	0.7018027	1.59652×10^{-7}
2	yes	no	1.945584	0.2766867	-0.2204121	1.221744	2.108025×10^{-5}
3	yes	yes	1.250418	0.2911026	-0.2090553	2.020853	5.145687×10^{-5}
4	no	yes	1.656492	0.3559866	-0.1269484	1.725476	3.215026×10^{-5}

Table 7: Parameter estimation results. *Logistic* closure model.

attempting RMSE evaluations with $\rho < 0$. For two η's (Table 4), $\sqrt{\rho}$ was used as the optimization variable to avoid this. The single-η model behaved somewhat better, although some local optima were found, with very small ρ, and RMSE quite close to those in Table 5. This, and the variability in parameter estimates across criteria, suggest some overparametrization, with ill-defined RMSE minima. For future work it would be advisable to start with the most parsimonious model, below, gradually freeing additional parameters.

The RMSE show little loss of fit by using a common η, especially for the interval predictions. Models were fitted also constraining the η for natural to be 1.5 and 2 times that for planted stands. As expected, forcing η to be larger for natural stands gave somewhat higher RMSE's, but not by much. Considering the apparent overparametrization it was decided to use a common η. Calculation of AIC and BIC values, below, also favoured the simpler model.

Results for the *linear* and *logistic* variants are shown in Tables 6 and 7,

Crit.	Interval	Weights	RMSE	α	η	ρ
1	no	no	3.008798	0.5269854	8.574327	1.586917×10^{-7}
2	yes	no	1.923116	0.5344907	10.34954	1.815103×10^{-6}
3	yes	yes	1.21652	0.5512178	11.66982	1.620877×10^{-6}
4	no	yes	1.642991	0.5323236	9.903429	5.025795×10^{-6}

Table 8: Parameter estimation results. emphLinear closure model with $\beta = 0$

respectively. The *linear* was superior to the *logistic* for all the criteria. The increase in RMSE relative to the *flexible* was relatively small. Convergence was reliable, and parameter differences across criteria are smaller than in the *flexible* model.

Finally, the *linear* variant was fitted forcing $\beta = 0$, with little effect on the predictions (Table 8).

4.3 Evaluation

4.3.1 Choosing the model form

The RMSE is expected to increase as the number of free parameters is reduced, so that they are not directly comparable. Although in some instances above the differences are negligible, pointing to a superiority of the simpler model. A popular way of discriminating between such models is to compute the Akaike Information Criterion (AIC), that penalizes complexity. A similar statistic is Schwartz's Bayesian Information criterion (BIC). Assuming independent normal residuals, the AIC and BIC can be calculated from the RMSE, the number of parameters λ, and the number of observations n as

$$2 \ln \mathrm{RMSE} + a\lambda \,,$$

where $a = 2$ for the AIC, and $a = \ln n$ for the BIC (e.g., R Development Core Team, 2009; Venables and Ripley, 2002, p. 174). Thes values are defined only up to an arbitrary additive constant, so that only differences are meaningful. Of course, the distributional assumptions are not really "true" (all models are wrong!), but these indices should still be useful for comparison, at least with criteria 2 and 3.

Table 9 gives the fit statistics for the various model forms, model complexity decreasing from left to right. The *logistic* is ommitted, because the RMSE was consistently higher than that of the *linear*, with the same number of parameters. Remember that only differences in AIC or BIC within a

	Flexible, two η's			Flexible, one η			Linear, free β			Linear, $\beta = 0$		
Crit.	RMSE	AIC	BIC	RMSE	AIC	BIC	RMSE	AIC	BIC	RMSE	AIC	BIC
1	2.925	**314.7**	332.4	2.978	317.8	332.5	2.994	317.3	329.1	3.009	316.6	**325.5**
2	1.913	195.0	212.7	1.919	193.8	208.5	1.919	191.9	203.7	1.923	**190.4**	**199.3**
3	1.213	66.5	84.2	1.213	64.6	79.3	1.216	63.2	75.0	1.217	**61.3**	**70.1**
4	1.587	**142.2**	159.9	1.631	147.9	162.7	1.642	147.8	159.6	1.643	146.0	**154.9**

Table 9: Root mean square eror, AIC, and BIC statistics for four model forms. Boldface indicates "best" (see text).

same row are meaningful, and smaller is better. The AIC is best for the *linear* model with $\beta = 0$ fitted by the interval criteria, but better for the most complex model when predicting from breast-height. The BIC, which penalizes complexity more heavily, consistently favours the most parsimonious model.

As mentioned before, the model with separate η's does not make biological sense, the differences in η for planted and natural stands being of the wrong sign. It seems clear also that it is overparametrized, with different combinations of parameter values resulting in essentially the same RMSE. Excluding this model, the AIC becomes consistently lowest in the *linear* $\beta = 0$ variant. It is seen also that the RMSE improves little by allowing a more general $\beta \neq 0$, or by going to the more complex *flexible* closure model. Prediction calculations show differences among models that are practically negligible. The $\beta = 0$ agrees with the preliminary analysis of Section 3.3.2.

Therefore, the *linear* model form with $\beta = 0$ was chosen. It seems remarkable that such a simple model describes well the basal area dynamics, with only two free parameters (not counting ρ, that enters in the initialization). It should be interesting to investigate the relationships with more extensive dada from other species.

4.3.2 Choosing the criteria

As indicated the criteria RMSE's are not comparable. As a way of assessing performance across the board, each set of parameters was used to compute the RMSE according to the other 3 criteria. Table 10 shows for each criterion (column), the difference in RMSE as a percentage of the best solution. In general, the lack-of-fit for criteria different from the one used in estimation seems acceptable. Fitting criteria 2 shows up as slightly more robust than the others, and criteria 1 as the least robust.

To compare further the 4 criteria, and to check for biases, graphs of residuals were prepared, the ones for the chosen model *linear*, $\beta = 0$ are shown in Figures 7–10. The residuals correspond to each measurement in every

	RMSE criteria							
	Flexible model				*Linear*, $\beta = 0$			
Fitting criteria	1	2	3	4	1	2	3	4
1	–	6.1	15.5	3.5	–	1.1	4.3	0.7
2	3.2	–	1.8	1.8	0.9	–	1.4	0.3
3	4.7	1.8	–	2.6	2.7	1.1	–	1.6
4	1.1	2.3	4.0	–	0.5	0.2	1.9	–

Table 10: Percentage RMSE differences for each criterion

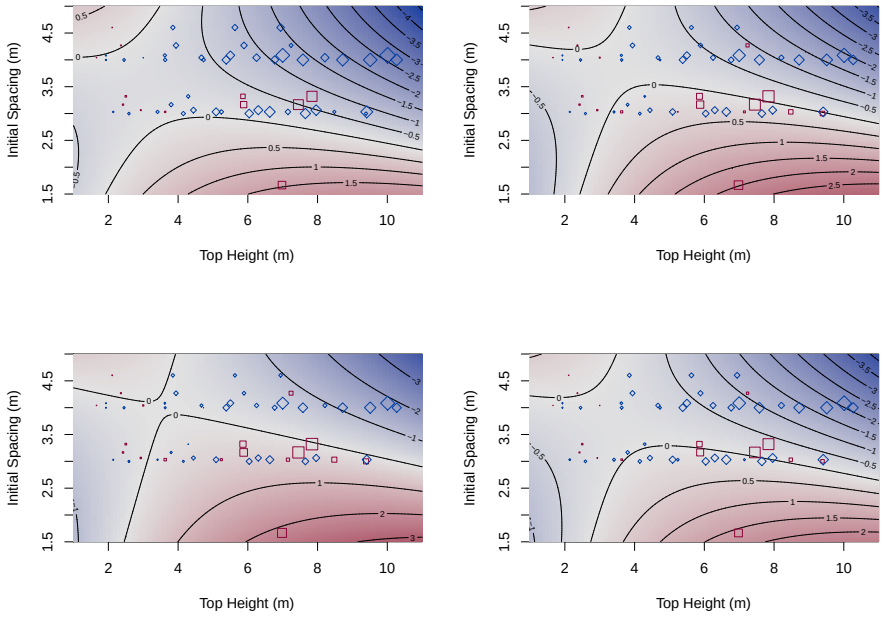

Figure 7: Residuals for projections from breast height, young plots. Fitting criteria 1 to 4, by rows from top. Symbol area is proportional to the residual, red squares for negative, and blue diamonds for positive. Contour lines and shading correspond to a quadratic surface fitted to the residuals.

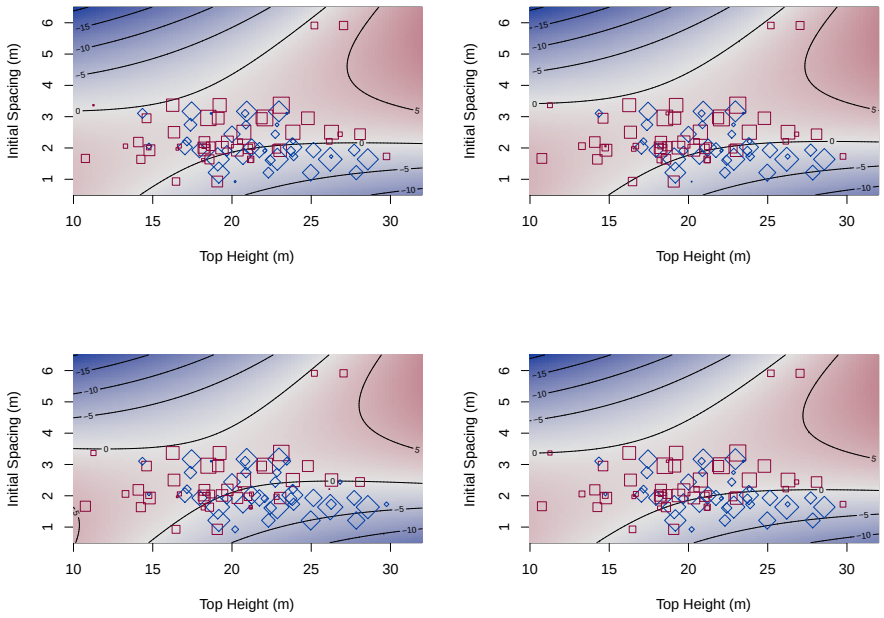

Figure 8: As Figure 7, for older plots.

plot, plotted over the plot estimated initial density and the measurement top height. Quadratic surfaces were fitted to the residuals by least-squares. There are no obvious systematic biases, and no clear differences among criteria.

Figure 11 shows the predicted bounds for full-occupancy trajectories $BHN^{-k} = x(H)$, see (8) and (15). Actual trajectories would be parallel to these, but displaced to the right, depending on initial density. They do not look unreasonable, with TT (criterion 3) a little different from the others.

.

.

The predicted increase in occupancy $\Omega = F[x(H) + C]$ is graphed in Figures 12 and 13, starting with 2000 stems per hectare, for the *flexible* / power and *linear* / $\beta = 0$ models. Comparing fitting criteria, the curves for criterion 1, and also criterion 3 in Fig. 12, are a little different from the rest. The occupancy trends are as might be expected, and are similar for both models. Differences in basal area or volume predictions, obtained from

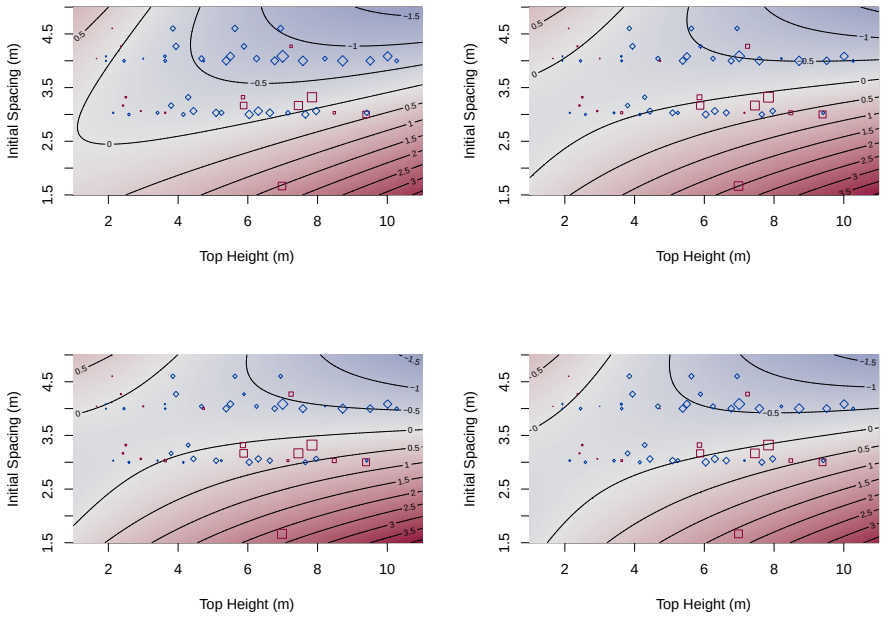

Figure 9: Residuals for shortest-interval predictions, young plots (cf. Figure 7).

integretion, are much less apparent.

Finally, observed and predicted basal area – age trajectories were graphed for the 4 fitting criteria, using both predictions from breast height and from the previous measurement (e.g., Figure 14). All models looked fairly similar.

Over all, prediction differences among the fitting criteria were paractically negligible, but te estimates from criterion 2 were chosen as being slightly more "middle-of-the-road". The final model, therefore, uses (25), $\beta = 0$, and the parameters on line 2 of Table 8.

4.3.3 Residuals and prediction accuracy

Figure 14 displays interval predictions, compared to the observed values. A popular way of evaluating model bias and precision is to graph observed over predicted values (e.g., Vanclay and Skovsgaard, 1997), and this has been done in Figure 15 for predictions from breast height. It may be argued

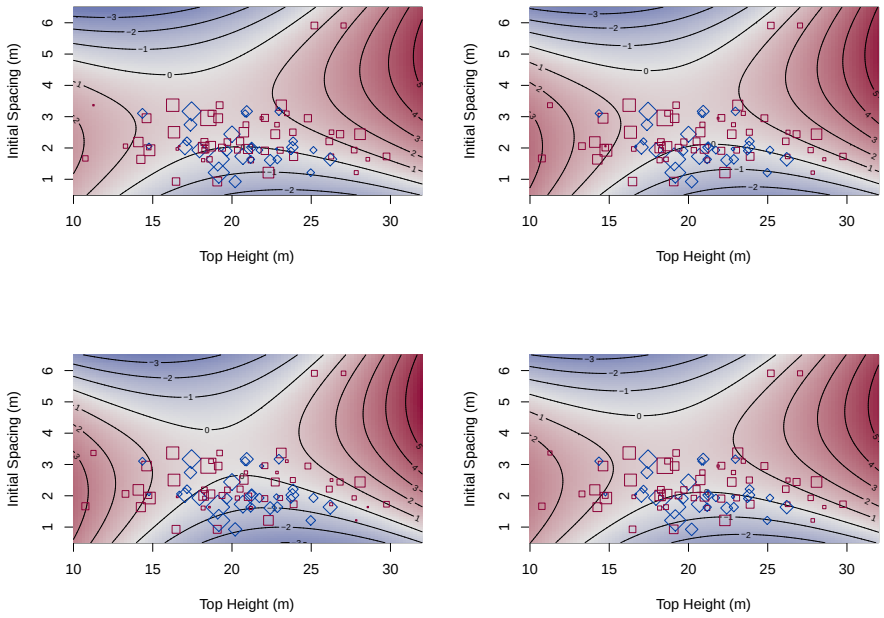

Figure 10: As Figure 9, for older plots.

Variable	Mean	Age < 25 Mean Deviation %	Age < 25 Mean Abs. Deviation %	Age < 25 RMSE %	Mean	Age > 25 Mean Deviation %	Age > 25 Mean Abs. Deviation %	Age > 25 RMSE %
H	5.37	0.81	4.26	5.16	20.6	-0.077	1.95	2.43
N	780.8	-4.11	4.11	6.14	1733	0.255	6.59	11.3
B	3.61	-6.45	18.7	30.7	35.8	1.296	8.56	10.6
V	10.8	-4.89	16.8	29.9	270	0.611	9.98	12.7

Table 11: Residual statistics for predictions from breast height

that this representation gives a rather optimistic visual impression, and a representation of residuals on the y-axis can be more useful. That is, plotting observed minus predicted, the vertical deviations from Figure 15. A graph of basal area residuals over age is shown in Figure 16, expressing the residuals as percentages of the observed value. No obvious biases are seen in either graph.

Table 11 gives an idea of the differences that can be expected in individ-

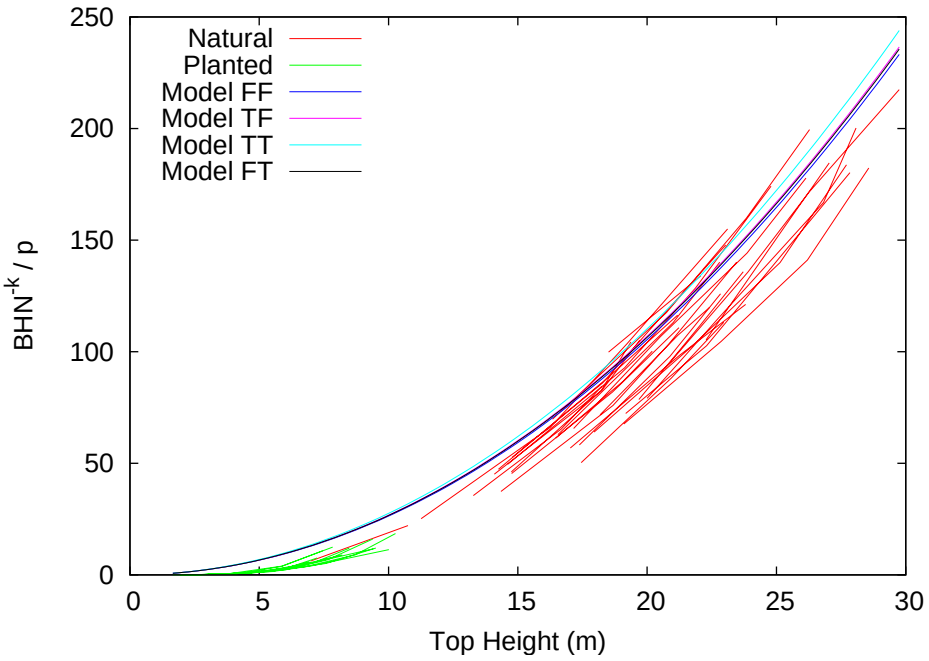

Figure 11: Highest full-occupancy trajectories (see text). Model fits designated according to if it used shortest intervals (True or False), and weighting. I.e., FF $\rightarrow$ criterion 1, TF $\rightarrow$ 2, TT $\rightarrow$ 3, FT $\rightarrow$ 4.

ual plot predictions. The statistics are for observed minus predicted, from breast height, using all the available measurements, and are tabulated as percentages of the mean. V is the total volume per hectare, see Section 6.

5 Was Eichhorn's assumption good enough?

To attempt answering this question, one may plot the residuals from the final model over site index or q, as in Figure 17.

At first sight, the decreasing trend seems to contradict Eichorn's hypothesis. A "significantly" negative linear regression coefficient can be calculated. However, the site index estimates are subject to error, with the extreme site index values likely to be outliers. If the lowest site indices are underestimates, the basal area is underestimated also, producing positive residuals. Similarly, negative residuals can be expected at the highest estimated site indices. This is an *error-in-variables* situation, where it is known that regressions are biased (Seber and Wild, 2003, Section 1.4).

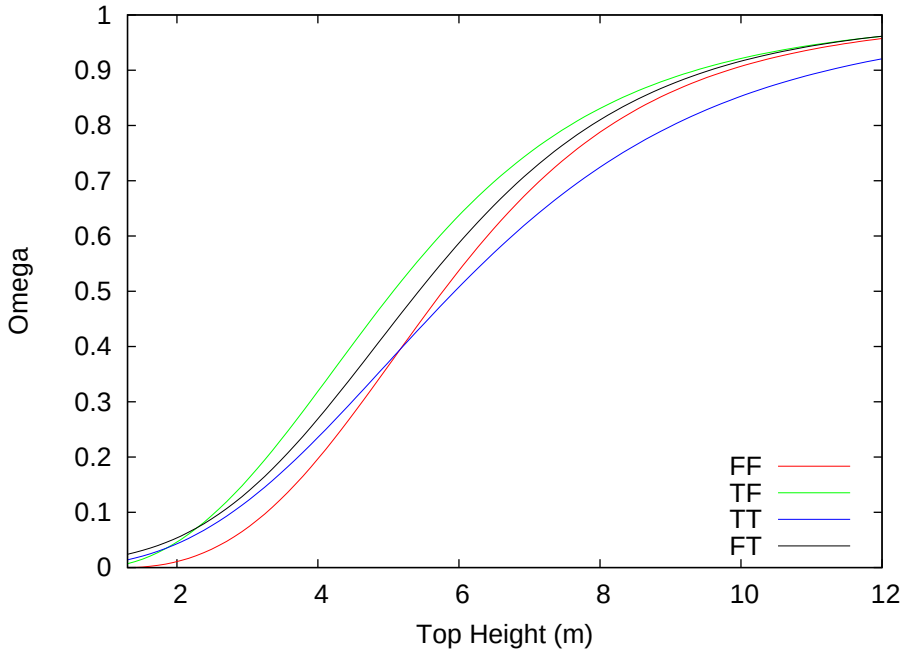

Figure 12: Occupancy predictions, starting from $N = 2000$. *Flexible*, $f(H) = H^{1-\beta}$. Fitting criteria labels as in Figure 11

With these data, a more elaborate analysis, possible with methods from Chapter 10 of Seber and Wild (2003), is likely to be unwarranted. But it seems clear from the Figure that any deviation from the hypothesis would be small compared to the prediction variability, at least ignoring the extremes.

6 Volumes, thinning

Volumes per hectare can be estimated given the state variables H, N, and B. Most stand volume tables use only H and B, but Beekhuis (1966) has pointed out that N should be included for volumes before and after thinning to be consistent. Hu (2008) used the permanent sample plot data, including single-measurement plots not used for growth modelling, to obtain the following volume/basal area ratio regression:

$$\frac{V}{B} = 0.2716 + 0.3370H + 6.5262\frac{H}{N} \tag{31}$$

($n = 252$, SE $= 0.3684$).

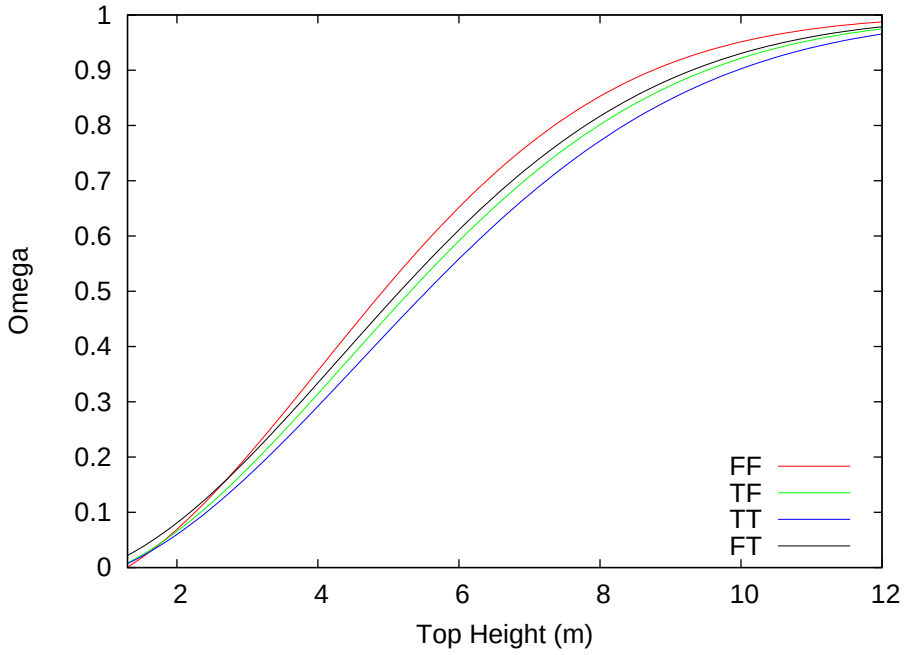

Figure 13: Occupancy predictions, starting from $N = 2000$. *Linear*, $\beta = 0$. Fitting criteria labels as in Figure 11

Equation (31) is of the same form as the one in García (2005), but the coefficients are considerably different. García (2005) used the TIPSY spruce data base, that was generated by simulation with the TASS growth model (Mitchell, 1975; Di Lucca, 1998; Mitchell *et al.*, 2004). For similar values of the state variables, the simulated plots have lower volumes than those observed in the SBS data (Figure 18). The reasons for the discrepancy are not clear, they may be due to different tree volume calculation procedures, or to differences between the simulated and observed tree size distributions. Equation (31) is used in the current model implementation.

Other useful relationships estimate merchantable to total volume ratios, and residual thinning basal areas from number of trees or vice-versa. Equations from García (2005) are being used.

7 Implementation

Various computer implementations of the mathematical model are possible. Three have been produced so far: (a) The R functions used for estimation

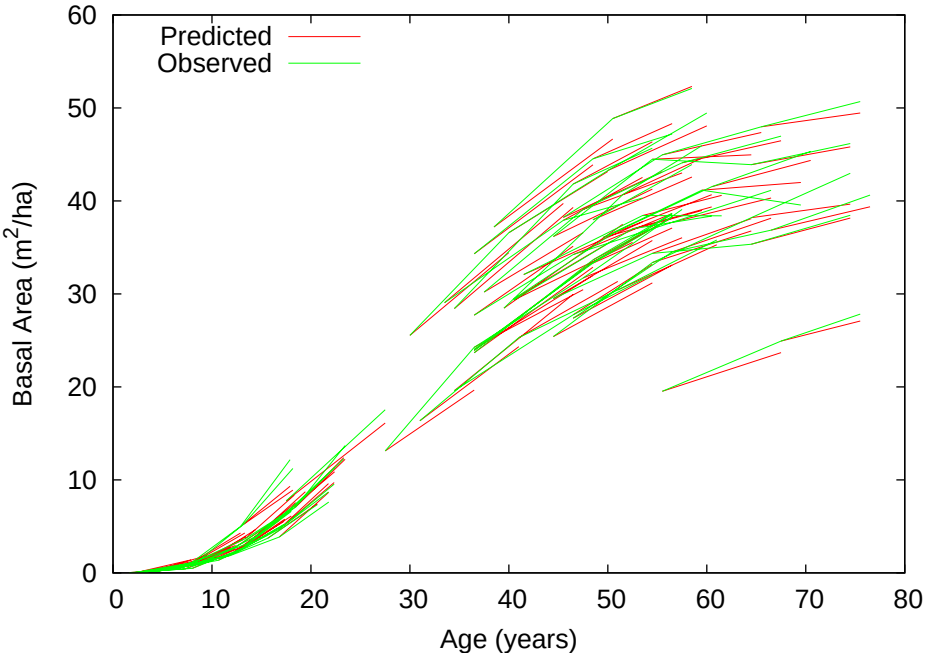

Figure 14: Increments predicted from the previous measurement.

and evaluation (Appendix C). (b) An interactive simulator in Microsoft Excel. (c) A System Dynamics box-and-arrow version in Vensim. Comparison of the outputs gives confidence in the correctness of the implementations. The model has been named "Scube", for the 3 S's in the title.

The Excel macros follow closely the equations and notation in this report. They are documented in the code, which is licensed as Open Source. A Help pdf file explaining usage and the main ideas behind the model is included in the package, which is available from `http://forestgrowth.unbc.ca/scube`.

The Vensim implementation carries out the direct numerical integration of the model differential equations, and is described in Appendix D. It is useful for checking and experimentation.

8 Comparison with existing models

Two other models are available for predicting spruce growth in the SBS:

TASS / TIPSY. TASS (Mitchell, 1975; Di Lucca, 1998) is a distance-

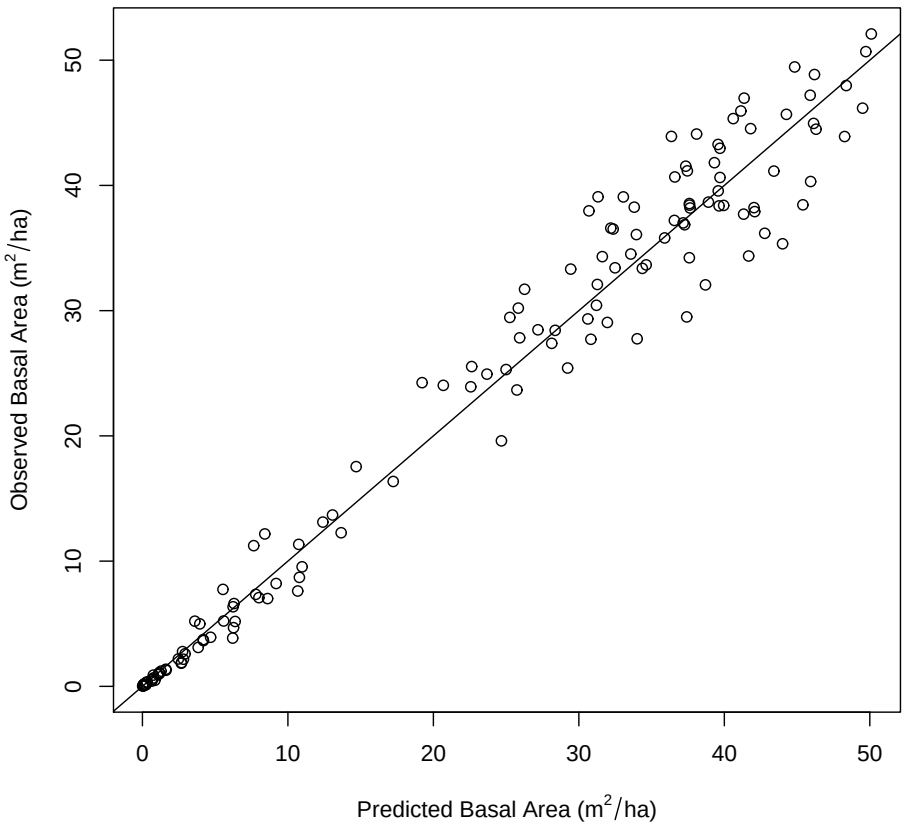

Figure 15: Observed and predicted basal areas. Predictions starting from breast height.

dependent individual-tree growth model for even-aged stands, with versions for various species on the Coast and the Interior of BC. The program is only available on the Ministry's computer system, so that it is commonly used indirectly through TIPSY, which is a look-up and interpolation system that accesses yield tables generated by TASS (Di Lucca, 1998; Ministry of Forests and Range, 2009a). Another alternative is TADAM (García, 2005), a dynamic stand-level (or whole-stand) approximation to the same yield tables.

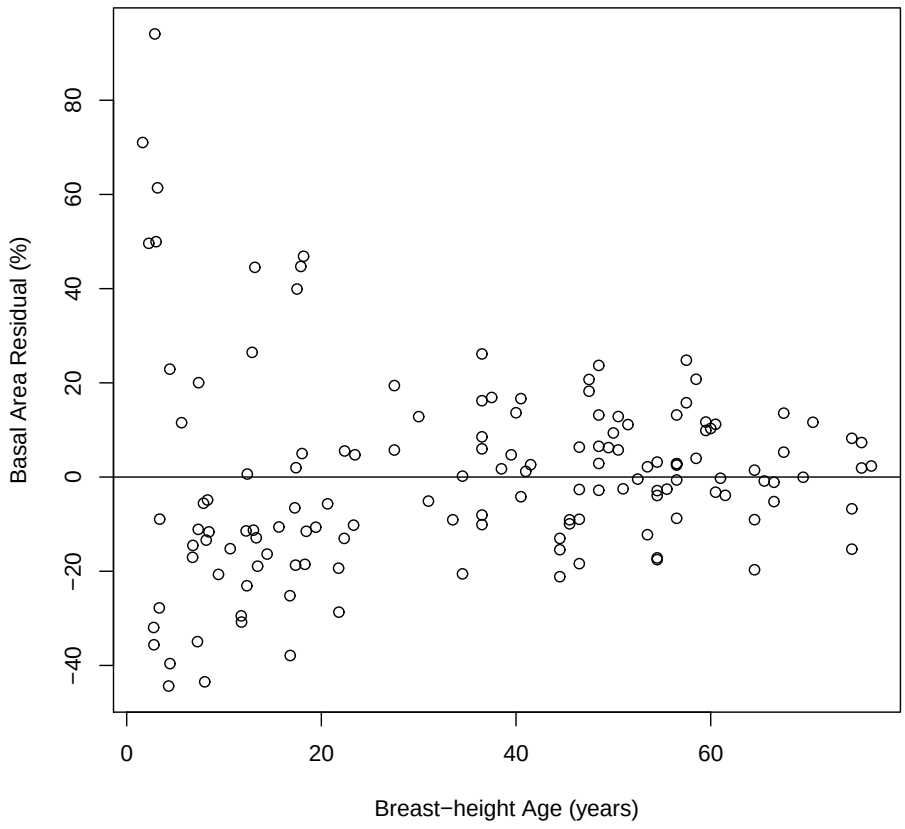

Figure 16: Relative basal area residuals, predictions from breast height.

VDYP 7. A whole-stand growth model for natural stands of various species in BC (Ministry of Forests and Range, 2009b). However, the option for projecting yields starting from bare land may not be working properly. The calculated basal areas and volumes were very low compared to the PSP data, and will not be discussed further here.

To illustrate the model predictions, two examples were simulated in Scube and TIPSY, for site index 20 (near average):

1. A planted stand of pure spruce, unthinned, starting with 1000 stems per hectare at breast height. This density is at the upper end of the

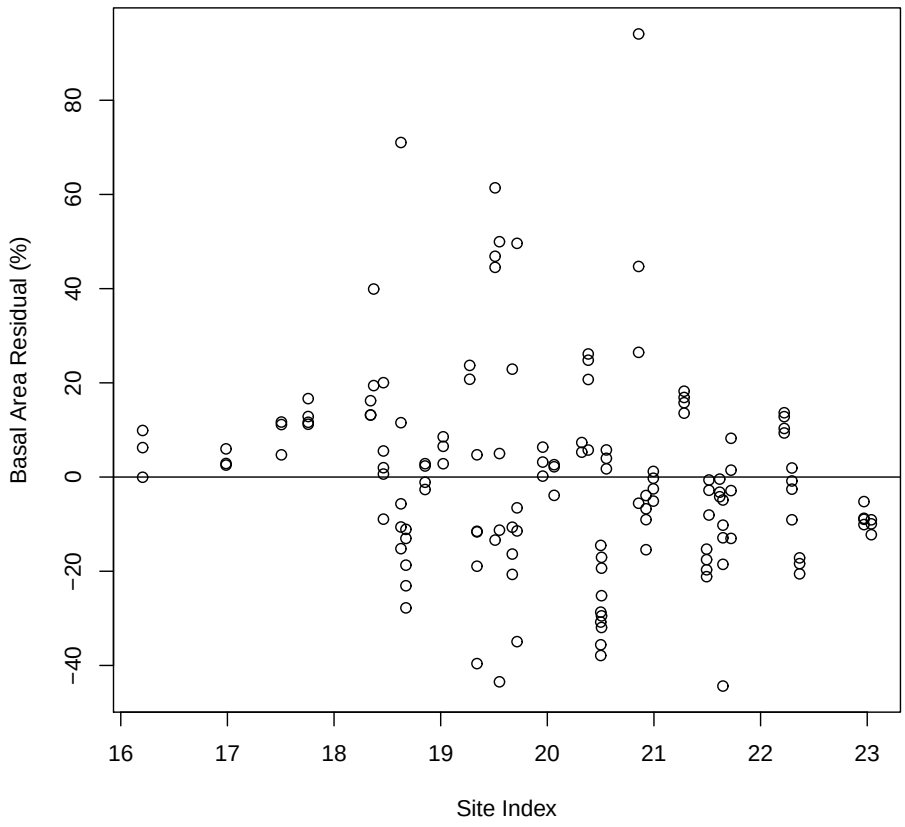

Figure 17: Relative basal area residuals over estimated plot site index. Predictions from breast height.

planted plots, but probably close to the minimum advisable under operational conditions. The latest TIPSY version 4.1d was used, with the program defaults. Simulation was straightforward with both programs.

2. A natural stand with 80% spruce by basal area and 2500 (spruce) stems per hectare at breast height, about average for the natural PSPs. Scube does not make a difference between planted and natural, other than species composition, and does not care about what the other

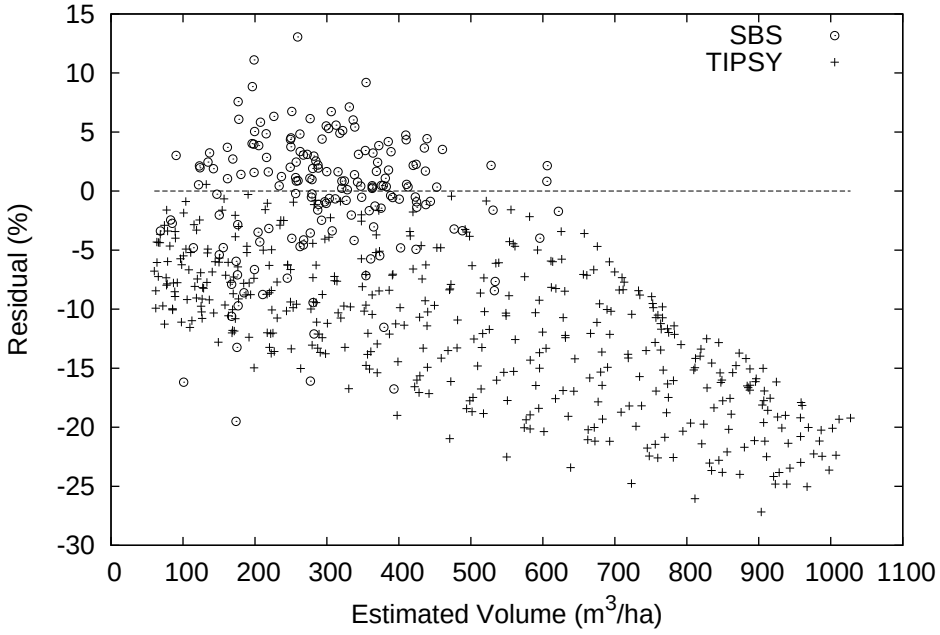

Figure 18: Residuals from model (31) for the SBS sample plot data, and the simulated plots in TIPSY

species might be. Of course, the number of years to breast height would be different, according to TIPSY 6 years from planting, or 11 years from germination or 13 since disturbance for the natural regeneration. TIPSY uses different tables for planted and natural, and projects only single-species stands. It does, however, have a facility for prorating mixed species yields, intended for forest-level planning and not for mixed species silviculture, but that we used as an approximation. The other 20% was assumed to be lodgepole pine, for which TIPSY used by default a slightly higher site index of 20.4. TIPSY reports totals per hectare, so it was assumed that 80% of the volumes and number of trees, as well as basal area, was spruce.

Results are shown in Figures 19–24, superimposed on the PSP data. For the higher-density natural stand, both models agree closely in the basal area and total volume predictions. Tipsy predicts higher mortality, and consequently larger tree sizes (Figs. 21 and 22), and higher merchantable volumes (not shown).

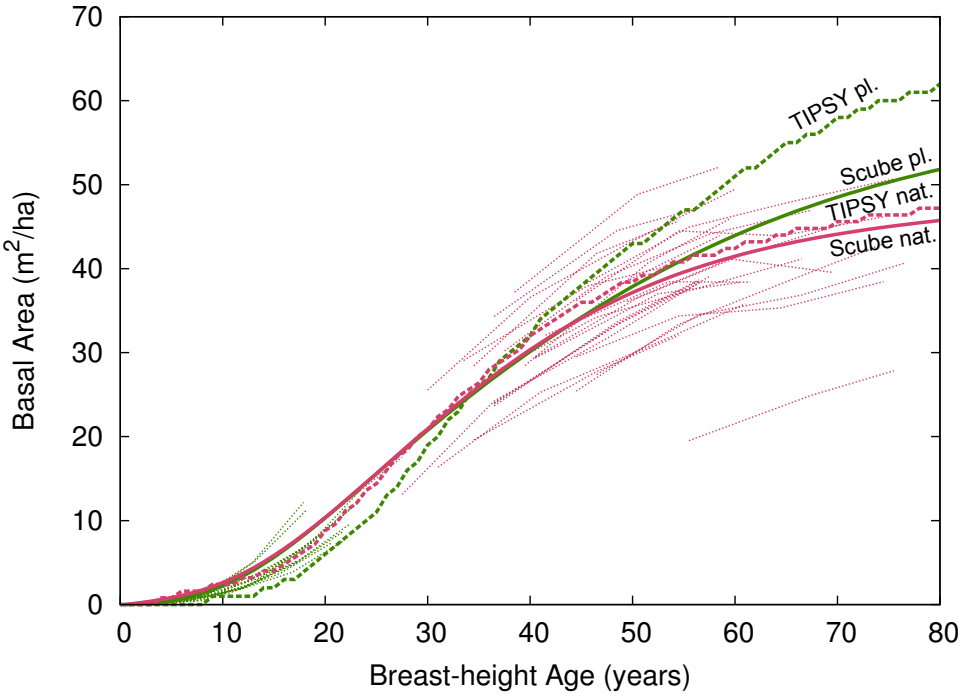

Figure 19: Basal area data and predictions with Scube and TIPSY. Planted is pure spruce, with initial density of 1000 sph. Natural is 80% spruce, initial density 2500 sph. In color, planted is green, and natural red.

TIPSY predictions are below the observed young plantation basal areas, volumes, and dbh. In the absence of data, both model predictions for mature planted stands are speculative.

Acknowledgments

The white spruce data was provided by the Forest Sciences Program, Research Branch, and by the Forest Analysis and Inventory Branch of the British Columbia Ministry of Forests and Range. It was screened and processed by Zhengjun Hu, as part of his Master of Science research at UNBC.

References

Assmann, E. 1970. The Principles of Forest Yield Study. Pergamon Press, Oxford, England, 506 p.

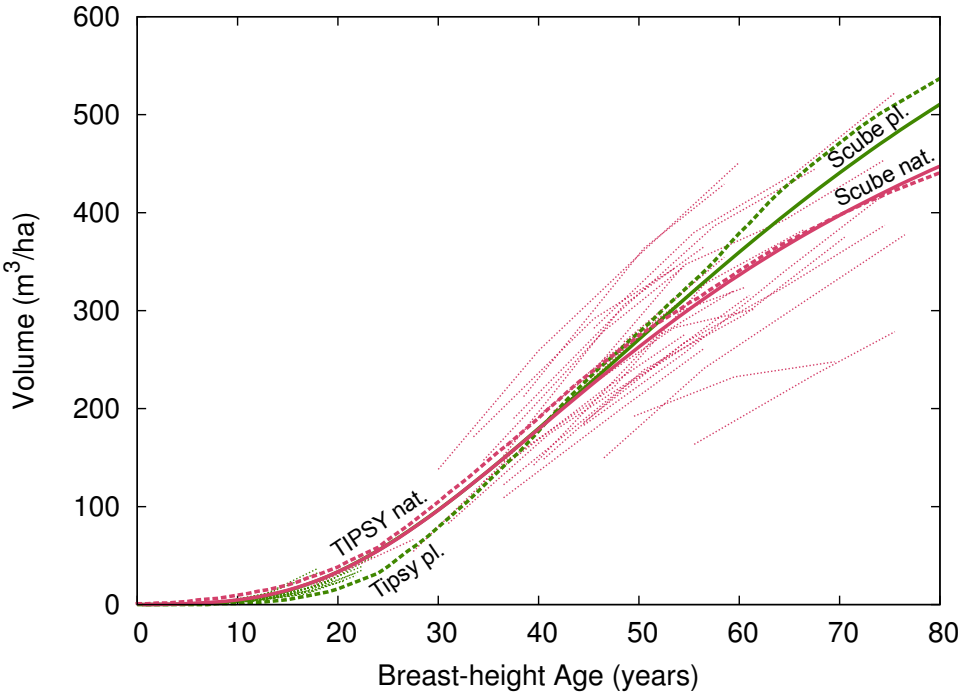

Figure 20: Total volume data and predictions with Scube and TIPSY.

Bard, Y. 1974. Nonlinear Parameter Estimation. Academic Press, New York.

Beekhuis, J. 1966. Prediction of yield and increment in *Pinus radiata* stands in New Zealand. Technical Paper 49, Forest Research Institute, NZ Forest Service.

Borders, B.E., Bailey, R.L., and Clutter, M.L. 1988. Forest growth models: Parameter estimation using real growth series. *In* Ek, A.R., Shifley, S.R., and Burk, T.E. (Editors), Forest Growth Modelling and Prediction, USDA Forest Service, General Technical Report NC-120, 660–667.

Buford, M., and Burkhart, H. 1987. Genetic improvement effects on growth and yield of loblolly pine plantations. Forest Science 33: 707–724.

Carson, S.D., Garcia, O., and Hayes, J.D. 1999. Realized gain and prediction of yield with genetically improved *Pinus radiata* in New Zealand. Forest Science 45: 186–200.

Di Lucca, C.M. 1998. TASS/SYLVER/TIPSY: systems for predicting the impact of silviculturalpractices on yield, lumber value, economic return

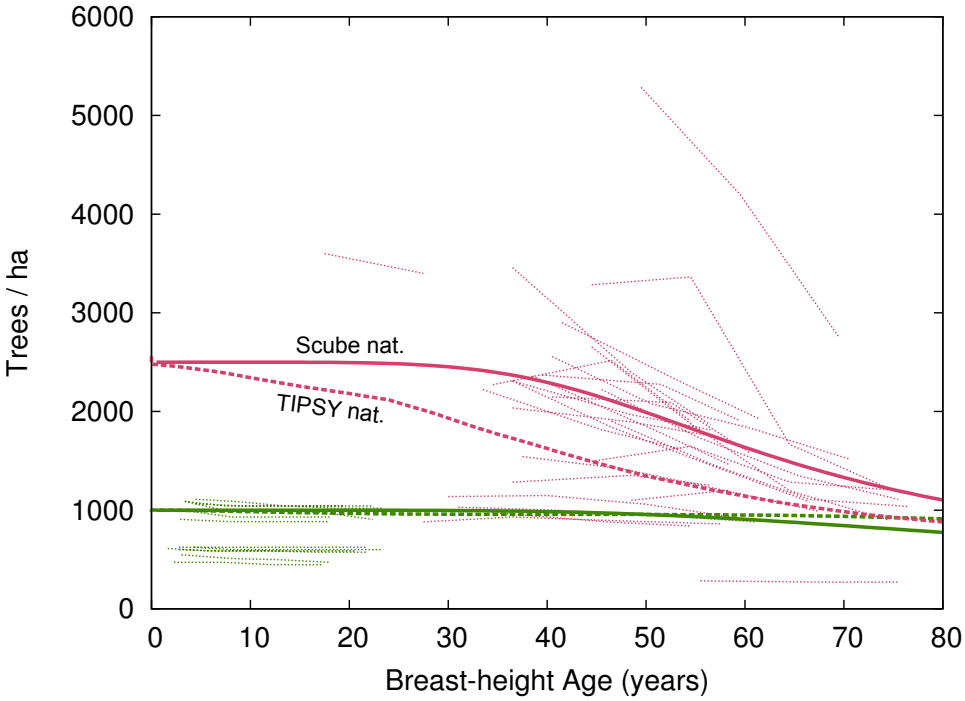

Figure 21: Stand density data and predictions with Scube and TIPSY.

and other benefits. *In* Bamsey, C.R. (Editor), Stand Density Management Conference: Using the Planning Tools. November23–24, 1987, Edmonton, Alberta, Alberta Environmental Protection, 7–16.

Eichhorn, F. 1904. Beziehungen zwischen Bestandshöhe und Bestandsmasse. Allg.Forst- u.Jagdztg. 80: 45–49.

García, O. 1989. Growth modelling — new developments. *In* Nagumo, H., and Konohira, Y. (Editors), Japan and New Zealand Symposium on Forestry Management Planning, Japan Association for Forestry Statistics, 152–158.

García, O. 1990. Growth of thinned and pruned stands. *In* James, R.N., and Tarlton, G.L. (Editors), New Approaches to Spacing and Thinning in Plantation Forestry: Proceedings of a IUFRO Symposium, Rotorua, New Zealand, 10–14 April 1989, Ministry of Forestry, FRI Bulletin No. 151, 84–97.

García, O. 2005. TADAM: A dynamic whole-stand approximation for the

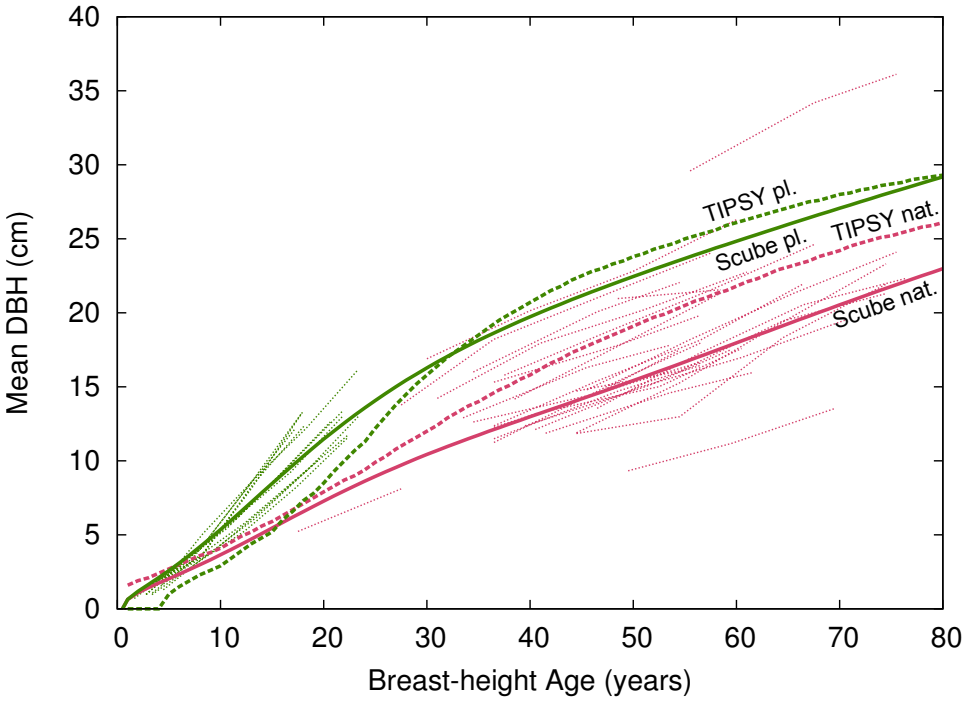

Figure 22: Quadratic mean dbh data and predictions with Scube and TIPSY.

TASS growth model. The Forestry Chronicle 81: 575–581, errata in 81: 815.

García, O. 2006. Site index: Concepts and methods. *In* Cieszewski, C.J., and Strub, M. (Editors), Second International Conference on Forest Measurements and Quantitative Methods and Management & The 2004 Southern Mensurationists Meeting, Warnell School of Forestry and Natural Resources, University of Georgia, Athens, GA, USA, 275–283.

García, O. 2008. Visualization of a general family of growth functions and probability distributions - the growth-curve explorer. Environmental Modelling & Software 23: 1474–1475.

García, O. 2009. A simple and effective forest stand mortality model. International Journal of Mathematical and Computational Forestry & Natural-Resource Sciences (MCFNS) 1: 1–9, `http://mcfns.com/index.php/Journal/article/view/MCFNS-1:1/44`.

García, O., and Ruiz, F. 2003. A growth model for eucalypt in Galicia,

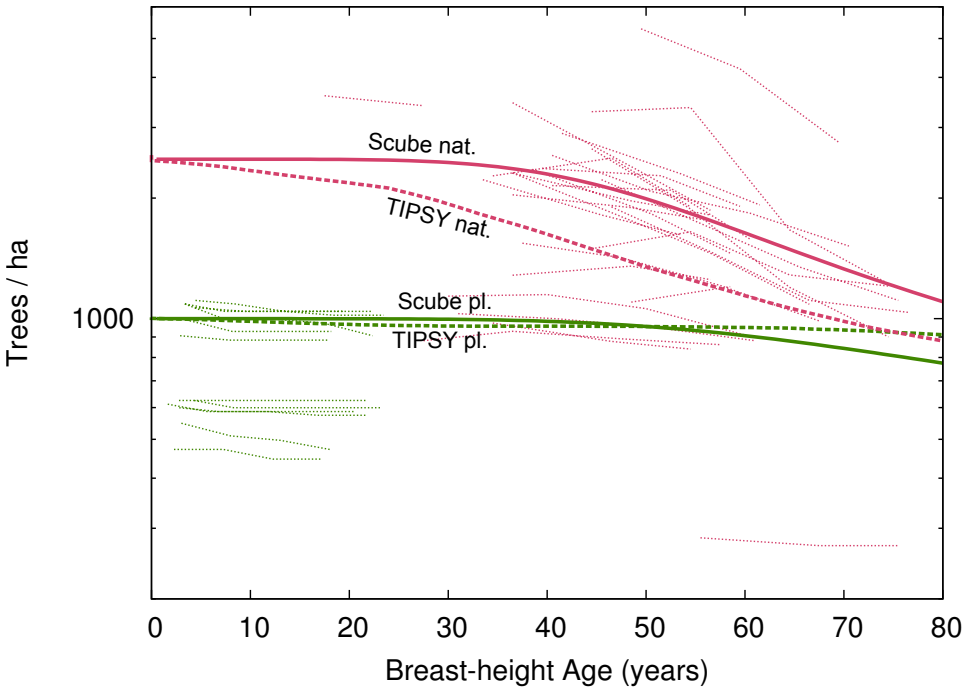

Figure 23: Stand density data and predictions with Scube and TIPSY, logarithmic scale.

Spain. Forest Ecology and Management 173: 49–62, errata at `http://web.unbc.ca/~~garcia/publ/publs.htm`.

Goulding, C.J. 1979. Validation of growth models used in forest management. New Zealand Journal of Forestry 24: 108–124.

Hale, S.E. 2003. The effect of thinning intensity on the below-canopy light environment in a Sitka spruce plantation. Forest Ecology and Management 179: 341?349.

Hu, Z. 2008. Developing a Whole-Stand Growth Model for Interior Spruce in the SBS Zone of British Columbia with Stochastic Differential Equations. Master thesis (draft), University of Northern British Columbia.

Ministry of Forests and Range 2009a. Tipsy home page, `http://www.for.gov.bc.ca/hre/gymodels/TIPSY/` (Accessed July 2009).
URL: *http://www.for.gov.bc.ca/hre/gymodels/TIPSY/*

Ministry of Forests and Range 2009b. Vdyp home, `http://www.for.gov.`

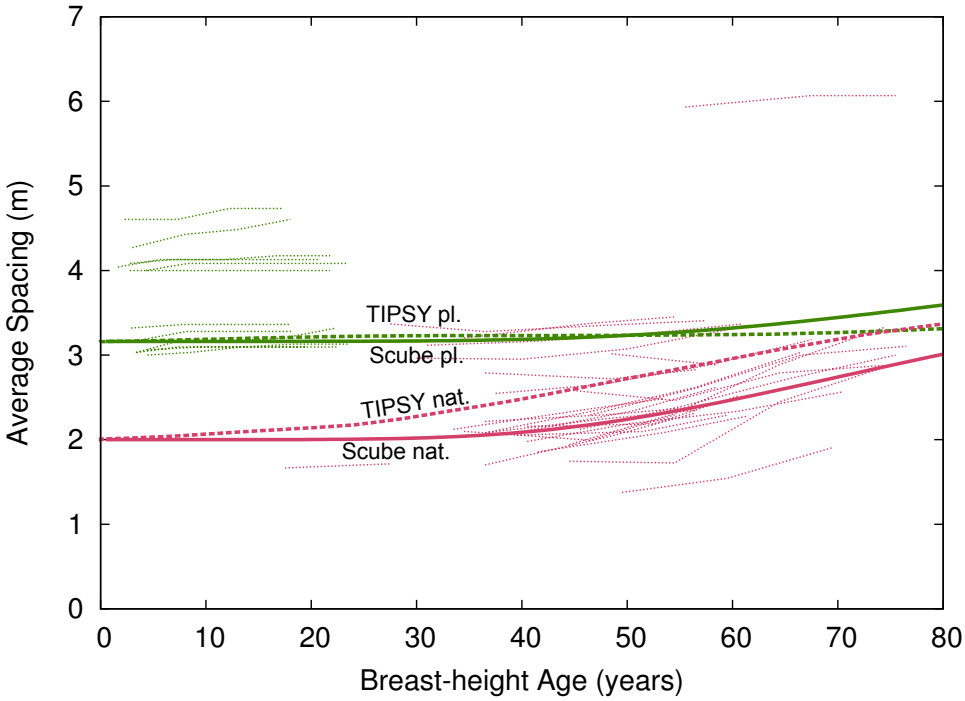

Figure 24: Average spacing data and predictions with Scube and TIPSY.

`bc.ca/hts/vdyp/` (Accessed July 2009).
URL: *http://www.for.gov.bc.ca/hts/vdyp/*

Mitchell, K.J. 1975. Dynamics and simulated yield of Douglas-fir. Forest Science Monograph 17, Society of American Foresters.

Mitchell, K.J., and Cameron, I.R. 1985. Managed stand yield tables for coastal Douglas-fir: Initial density and precommercial thinning. Land Management Report 31, B. C. Ministry of Forests, Research Branch, Victoria, British Columbia.

Mitchell, K.J., Stone, M., Grout, S.E., Di Lucca, C.M., Nigh, G., Goudie, J.W., Stone, J.N., Nussbaum, A.J., Stearns-Smith, A.Y.S., and Brockley, R. 2004. TIPSY Version 3.2. B. C. Ministry of Forests, Research Branch, Victoria, B. C.

Newnham, R.M. 1964. The Development of a Stand Model for Douglas Fir. Ph.D. thesis, The University of British Columbia.

R Development Core Team 2009. R: A Language and Environment for Statistical Computing. R Foundation for Statistical Computing, Vienna, Austria, ISBN 3-900051-07-0.
URL: *http://www.R-project.org*

Seber, G.A.F., and Wild, C.J. 2003. Nonlinear Regression. Wiley-Interscience, New York, 768 p.

Staebler, G.R. 1951. Growth and Spacing in an Even-aged Stand of Douglas-Fir. Master's thesis, School of Natural Resources, University of Michigan.

Vanclay, J., and Skovsgaard, J. 1997. Evaluating forest growth models. Ecological Modelling 98: 1–12.

Vanclay, J.K. 1994. Modelling Forest Growth and Yield: Applications to Mixed Tropical Forests. CABI International, Wallingford, UK, 312 p. (`http://espace.library.uq.edu.au/eserv/UQ:8211/ModellingForestG.pdf`).

Venables, W.N., and Ripley, B.D. 2002. Modern Applied Statistics with S. Springer, New York, fourth edition, 495 p.

A p-dependent mortality model

It would seem more consistent to account for species composition when predicting mortality. This might be done simply by substituting N/p for N in the model equations. The following model was obtained:

$$(S\sqrt{p})^{3.682} - (0.06554H)^{5.703} = \text{constant} \; . \tag{32}$$

The residual standard error for $\ln S$ was 0.04197, compared to 0.04091 for the original model.

Re-estimation of the basal area model for criterion 3 resulted in a RMSE of 1.418, slightly worse than the original 1.407.

B Planted *vs.* natural

This is a simplistic modelling investigation to explore and demonstrate expected differences in closure/occupancy efficiency between natural and planted stands. We do not distinguish here between closure and occupancy. Natural stands are represented by a random tree location pattern, while plantations have a regular one.

Assume N trees per hectare, each with a circular zone of influence (ZOI) of area z. Consider two cases:

Random. Tree locations are Poisson.

Regular. Tree locations on a regular square grid.

We are interested in the growth with z of the occupancy Ω, defined as the proportion of area occupied by the union of the ZOIs. Also in its integral $G(z) = \int_0^z \Omega \, \mathrm{d}z$, and the "rounded ramp" function $z - G(z)$. Might assume that z increases linearly with H (Figure 25).

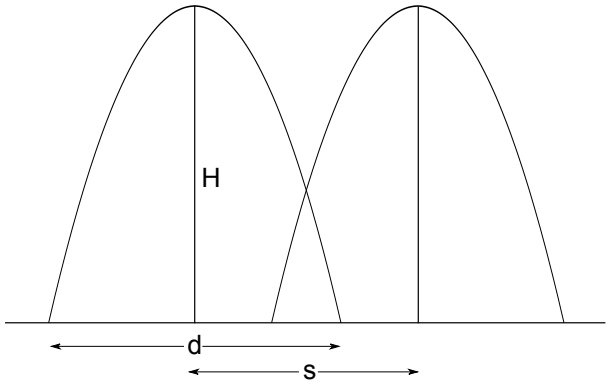

Figure 25: Parabolic ZOI.

B.1 Random

Consider an area A, containing $n = NA$ trees. $1 - \Omega$ is the proportion of the area not covered by any of the n ZOIs. The probability of a point not being in a ZOI is $1 - z/A$. Since the locations are independent,

$$E(1 - \Omega) = (1 - z/A)^n = (1 - z/A)^{NA} \, .$$

As A increases,

$$1 - \Omega = \lim_{A \to \infty} (1 - z/A)^{NA} = \mathrm{e}^{-Nz} \, .$$

Therefore,

$$\Omega = 1 - \mathrm{e}^{-Nz} \, . \tag{33}$$

The integral is

$$G(z) = \int_0^z (1 - \mathrm{e}^{-Nx})\,\mathrm{d}x\ ,$$

$$G(z) = z - (1 - \mathrm{e}^{-Nz})/N\ . \tag{34}$$

The ramp is

$$z - G(z) = (1 - \mathrm{e}^{-Nz})/N\ . \tag{35}$$

The ramp asymptote is 1, and the value at $Nz = 1$ is $(1 - 1/\mathrm{e})/N \approx 0.6321/N$.

B.2 Regular

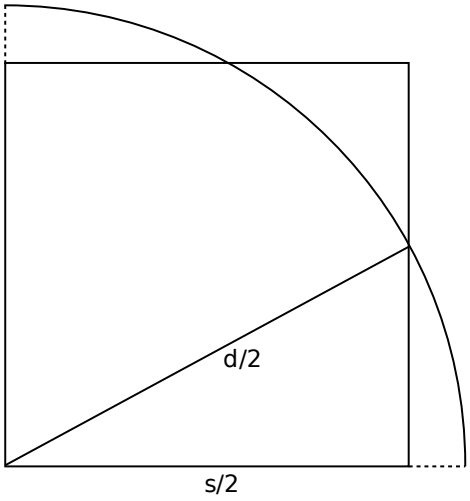

Figure 26: Occupancy for square spacing, $\pi/4 \le Nz \le \pi/2$.

Let $s = 1/\sqrt{N}$ be the average spacing, and d the ZOI diameter, $z = \pi d^2/4$. The ZOIs do not touch until $d = s$, so that $\Omega = Nz$ for $d \le s$. Occupancy is complete for $d \ge \sqrt{2}s$ (Figure 26). In-between, from the geometry of Figure 26 it its found that

$$\begin{aligned}\Omega &= \frac{\pi(d/2)^2/4 - 2[(d/2)^2 \arccos(s/d)/2 - (s/2)\sqrt{(d/2)^2 - (s/2)^2}/2]}{(s/2)^2} \\ &= \pi(d/s)^2/4 - (d/s)^2 \arccos(s/d) + \sqrt{(d/s)^2 - 1}\ .\end{aligned}$$

Therefore, substituting $(d/s)^2 = 4Nz/\pi$,

$$\Omega = \begin{cases} Nz & \text{if } Nz \le \pi/4, \\ Nz - 4Nz \arccos \sqrt{\pi/(4Nz)}/\pi + \sqrt{4Nz/\pi - 1} & \text{if } \pi/4 \le Nz \le \pi/2, \\ 1 & \text{if } Nz \ge \pi/2. \end{cases} \tag{36}$$

The integral is

$$G(z) = \begin{cases} Nz^2/2 & \text{if } Nz \le \pi/4, \\ (10z - \pi/N)\sqrt{4Nz/\pi - 1}/12 - Nz^2/2 & \\ \quad + 2Nz^2 \arcsin \sqrt{\pi/(4Nz)}/\pi & \text{if } \pi/4 \le Nz \le \pi/2, \\ z - \pi/(6N) & \text{if } Nz \ge \pi/2, \end{cases} \tag{37}$$

and the ramp is $z - G(z)$.

The ramp asymptote is $\pi/(6N) \approx 0.5236/N$, and the value at $Nz = \pi/6$ as a fraction of the asymptote is 0.7382.

B.3 Graphs and approximation

Figures 27, 28 and 29 show the various curves for both random (lower) and regular (upper). Figure 29 shows also the model

$$z - G(z) = \eta[1 + (z/\eta)^{-1/\theta}]^{-\theta}$$

that coincides with the curves at $z = \eta$. The coefficients are:

	η/N	θ
Random	1	0.6617
Regular	0.5236	0.4379

B.4 Postscript

See Figure 6 for an illustration. The ZOI fractions Nz are 0.5, 1.0, and 1.5. The numbers above each diagram are the corresponding Ω.

The above might suggest that the closure/occupancy rate equations should include N. However, the dependence on N disappears if the growth in ZOI varies with the occupancy (which may or may not be a good assumption). I.e.,

$$\frac{\mathrm{d}Nz}{\mathrm{d}x} = f(\Omega) \; .$$

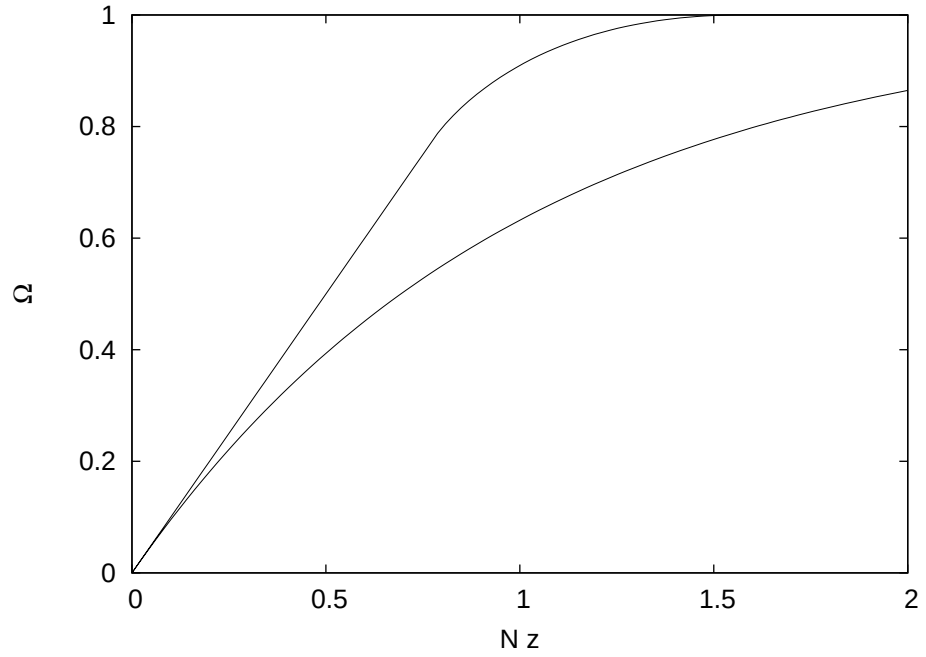

Figure 27: Occupancy for random locations (lower curve), and for square planting (upper curve).

We had $\Omega = F(Nz)$, given by (33) and (36). Then,

$$\frac{\mathrm{d}\Omega}{\mathrm{d}Nz} = F'(Nz) = F'[F^{-1}(\Omega)] \equiv g(\Omega) \; .$$

Or, solving first for Nz,

$$\frac{\mathrm{d}\Omega}{\mathrm{d}Nz} = 1/(\mathrm{d}Nz/\mathrm{d}\Omega) = 1/[F^{-1}(\Omega)]' \; .$$

For the random case, it is found that

$$\frac{\mathrm{d}\Omega}{\mathrm{d}Nz} = g(\Omega) = 1 - \Omega \; .$$

In the regular case it is not possible to write down an explicit expression for $g(\Omega)$, because (36) cannot be solved analytically for Nz.

Either way,

$$\frac{\mathrm{d}\Omega}{\mathrm{d}x} = \frac{\mathrm{d}\Omega}{\mathrm{d}Nz}\frac{\mathrm{d}Nz}{\mathrm{d}x} = g(\Omega)f(\Omega) \; . \tag{38}$$

For instance, if ZOI growth is proportional to occupancy, $f(\Omega) = \eta\Omega$, then in the random case Ω follows a logistic growth curve.

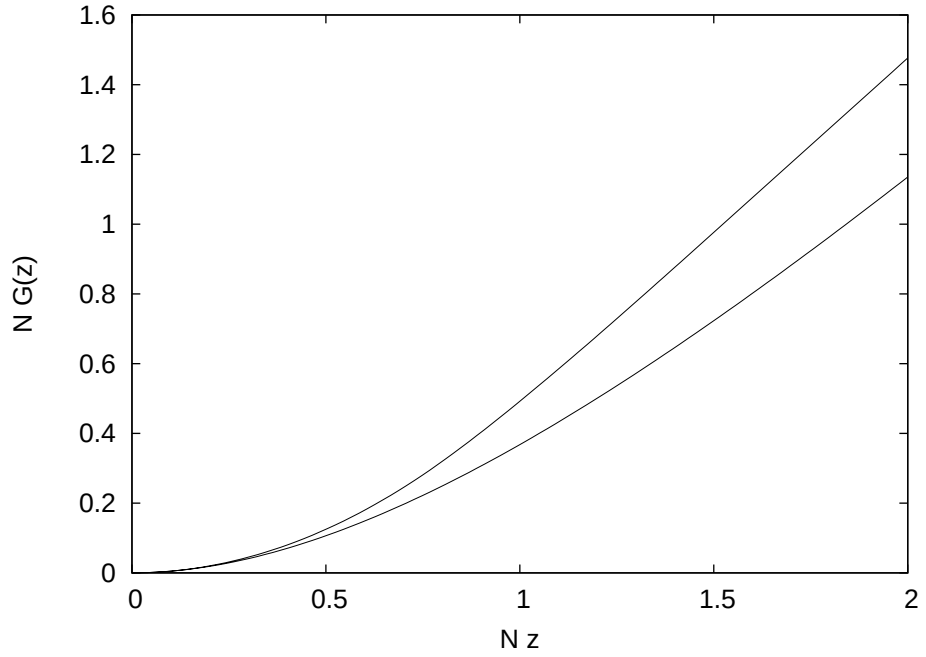

Figure 28: Integrated occupancy for random locations (lower curve), and for square planting (upper curve).

C Computer code

R functions used in parameter estimation and evaluation.

Invariant and state calculations, used in estimation and residual calculation procedures:

For the *flexible* closure model,

```
Invariants <- function(t, state, parameters, p, q, xpower)
# Calculate invariant vector y given time t, and state and parameters vectors.
#   state must have named elements H, N, R, and B.
#   parameters must have named elements alpha, beta, theta, eta, optionally k (default 0.3).
#   p is the proportion of spruce in the plot, by basal area.
#   q=b is the site quality parameter.
#   xpower=TRUE if f(H) is power function, or xpower=FALSE if f(H) is linear
{
    k = 0.3     # default
    attach(as.list(state))
    attach(as.list(parameters))
    y <- c()
    y[1] <- log(1 - (H / (283.87 * q^0.5137)) ^ 0.5829) + q * t
    y[2] <- (100 / sqrt(N)) ^ 3.979 - (0.07213 * H) ^ 6.009
    if (xpower) {
        x <- alpha * p * H ^ (2 - beta) / (2 - beta)
```

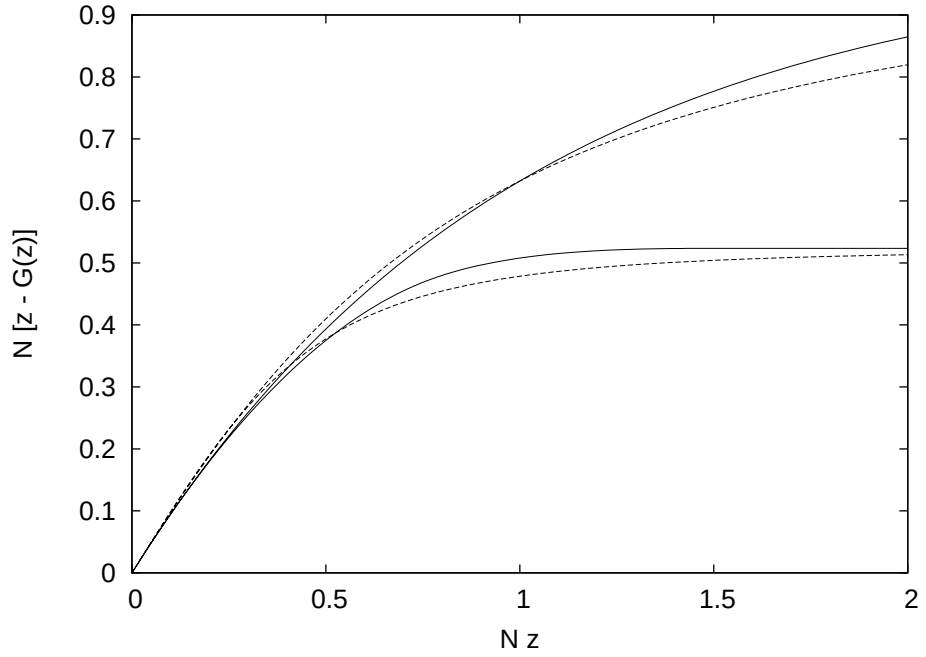

Figure 29: Accumulated loss from lack of occupancy for random locations (lower curve), and for square planting (upper curve). Dashed: ramp approximations.

```
    } else {
        x <- alpha * p * (H / 2 + beta) * H
    }
    if (R >= 1) {
        v <- eta
        y[3] <- 0
    } else {
        u <- (1 - R) ^ (2.2 / (theta + 1))
        v <- eta * (1 - u ) ^ theta
        y[3] <- u ^ theta / (v - u ^ theta * x)
    }
    y[4] <- B * H / N^k - x + v
    detach(as.list(state))
    detach(as.list(parameters))
    y
}
```

For the *linear* closure model, replace lines 24–26 by

```
u <- (1 - R) ^ 2.2
v <- eta * (1 - u )
y[3] <- u ^ exp(x / eta)
```

For the *flexible* closure model,

```
State <- function(t, y, parameters, p, q, xpower)
# Recover the state vector given time t, invariants vector y, and the parameters vector.
#   the returned state is a vector with named elements H, N, R, and B.
#   par has named elements alpha, beta, theta, eta, optionally k (default 0.3).
#   p is the proportion of spruce in the plot, by basal area.
#   q=b is the site quality parameter.
#   xpower=TRUE if f(H) is power function, or xpower=FALSE if f(H) is linear
{
    k = 0.3     # default
    parametersl <- as.list(parameters)
    attach(as.list(parameters))
    H <- (283.87 * q^0.5137) * (1 - exp(y[1] - q * t)) ^ (1/0.5829)
    N <- 10000 / (y[2] + (0.07213 * H)^6.009) ^ (2/3.979)
    if (xpower) {
        x <- alpha * p * H ^ (2 - beta) / (2 - beta)
    } else {
        x <- alpha * p * (H / 2 + beta) * H
    }
    if (y[3] == 0) {
        R <- 1
        v <- eta
    } else {
        u <- (eta * y[3] / (y[3] * x + 1)) ^ (1 / theta)
        u <- u / (u + 1)
        R <- 1 - u ^ ((theta + 1) / 2.2)
        v <- eta * (1 - u) ^ theta
    }
    B <- N^k * (y[4] + x - v) / H
    detach(as.list(parameters))
    c(H=H, N=N, R=R, B=B)
}
```

For the *linear* closure model, replace lines 23–26 by

```
    u <- y[3] / exp(x / eta)
    R <- 1 - u ^ (1 / 2.2)
    v <- eta * (1 - u)
```

Calculation of root mean squared error, objective function to be minimized in parameter estimation:

```
RMSE <- function(freePars, fixedPars=NULL, data, xpower, interval=TRUE, weighted=FALSE)
# Returns the basal area root mean squared error.
#   freePars is the vector of parameters to be optimized, fixedPars those fixed.
#   The parameters are in named elements alpha, beta, theta, eta, etaMult, rho,
#     and optionally k (default 0.3).
#   etaMult is the factor by which the planted eta is changed in natural stands.
#   The dataframe data must have columns named plot, sprucep, siteq, age, H, N, B.  Assumes increasing
#     age for each plot.
#   xpower=TRUE if f(H) is power function, or xpower=FALSE if f(H) is linear
#   If interval=TRUE, predictions are from the previous measurement (starting at breast height).
#   If interval=FALSE, predictions are from breast height.
#   If weighted=TRUE, squares are weighted by the reciprocal of the prediction interval.
{
    fail <- NA
#    fail <- 99  # L-BGFS-B requires finite value
    pars <- c(freePars, fixedPars)  # merge free and fixed parameters
```

```
if (any(!is.finite(pars))) {
    cat("\nBad parameters:", c(pars))
    return(fail)
}
if (any(pars[c("alpha", "theta", "eta", "etaMult", "rho")] <= 0)) {
    cat("\nNegative parameters:", c(pars))
    return(fail)
}
etaPl <- as.vector(pars["eta"])    # planted
etaNat <- etaPl * as.vector(pars["etaMult"])     # natural
ss <- sw <- 0    # initialize sum of squares and sum of weights
weight <- 1
for (plotID in unique(data$plot)) {     # loop over plots
    natural <-  plotID < 60     # planted stands have ID numbers > 60
    if (natural) {
        pars["eta"] <- etaNat
    } else {
        pars["eta"] <- etaPl
    }
    d <- data[data$plot == plotID,]     # dataframe for this plot
    n <- dim(d)[1]  # number of measurements
    p <- d$sprucep[1]
    q <- d$siteq[1]     # site parameter
    if (plotID != 23) {   # except for plot 23
        # initial state, at breast height
        N1 <- 10000 / ((100 / sqrt(d$N[1]))^3.979 - (0.07213 * d$H[1])^6.009 +
             (0.07213 * 1.3)^6.009) ^ (2/3.979)
        R1 <- pmin(as.vector(pars["rho"]) * N1, 1)
        state1 <- c(H = 1.3, N = N1, R = R1, B = 0)
        t1 <- 0.5   # age at breast height
    } else { # for plot 23, start from first measurement
        state1 <- c(H = d$H[1], N = d$N[1], R = 1, B = d$B[1])
        t1 <- d$age[1]
    }
    y <- Invariants(t1, state1, pars, p, q, xpower)
    for (i in 1:n) {    # measurements in plot
        if (plotID == 23 && i == 1) next   # for plot 23, skip first measurement
        t2 <- d$age[i]
        state2 <- State(t2, y, pars, p, q, xpower)
        if (weighted) {
            weight <- 1 / (t2 - t1)
        }
        ss <- ss + weight * (d$B[i] - as.vector(state2["B"])) ^ 2
        if (!is.finite(ss)) {
            cat("Abort, ss ", ss, " at plot ", plotID, ", meas ", i, ": " , c(pars))
            return(fail)
        }
        sw <- sw + weight
        if (interval && i < n) {
            state1["H"] <- d$H[i]
            state1["N"] <- d$N[i]
            state1["R"] <- as.vector(state2["R"])
            state1["B"] <- d$B[i]
            t1 <- t2
            y <- Invariants(t1, state1, pars, p, q, xpower)
        }
```

```
        } # end of plot
    } # end of data
    res = sqrt(ss / sw)
    return(res)
}
```

Example of parameter estimation call:

```
# Initial estimates:
guess <- c(alpha=0.6, theta=0.45, eta=15, etaMult=2.7,  rho=5e-5, beta=0)

# Free all parameters, power f(H). Interval, no weights

(power.int.nw <- optim(guess, RMSE, fixedPars=NULL, data=spruceData, xpower=T, interval=T,
 weighted=F, method="BFGS", control=list(parscale=c(guess[1:5],1), trace=1, REPORT=1, maxit=500)))
```

Predicted values:

```
Predictions <- function(pars, data, xpower, interval)
# For each data point returns the data frame, appending the predictions Hpred, Npred, R, Bpred.
#   Includes also the starting breast-height point, except for plot 23.
#   The parameters in pars are in named elements alpha, beta, theta, eta, etaMult, rho,
#     and optionally k (default 0.3).
#   etaMult is the factor by which the planted eta is changed in natural stands.
#   The dataframe data must have columns named plot, sprucep, siteq, age, H, N, B.  Assumes increasing
#     age for each plot.
#   xpower=TRUE if f(H) is power function, or xpower=FALSE if f(H) is linear
#   If interval=TRUE, predictions are from the previous measurement (starting at breast height).
#   If interval=FALSE, predictions are from breast height.
{
    out <- NULL
    etaPl <- as.vector(pars["eta"])    # planted
    etaNat <- etaPl * as.vector(pars["etaMult"])     # natural
    for (plotID in unique(data$plot)) {     # loop over plots
        natural <-  plotID < 60     # planted stands have ID numbers > 60
        if (natural) {
            pars["eta"] <- etaNat
        } else {
            pars["eta"] <- etaPl
        }
        d <- data[data$plot == plotID,]     # dataframe for this plot
        n <- dim(d)[1]  # number of measurements
        p <- d$sprucep[1]
        q <- d$siteq[1]     # site parameter
        if (plotID != 23) {   # except for plot 23
            # initial state, at breast height
            N1 <- 10000 / ((100 / sqrt(d$N[1]))^3.979 - (0.07213 * d$H[1])^6.009 +
                 (0.07213 * 1.3)^6.009) ^ (2/3.979)
            R1 <- pmin(as.vector(pars["rho"]) * N1, 1)
            state1 <- c(H = 1.3, N = N1, R = R1, B = 0)
            t1 <- 0.5   # age at breast height
            breastHt <- c(plotID, p, q, t1, 1.3, N1, 0)
        } else { # for plot 23, start from first measurement
            state1 <- c(H = d$H[1], N = d$N[1], R = 1, B = d$B[1])
            t1 <- d$age[1]
            breastHt <- NULL
        }
```

```
        pred <- data.frame(as.list(state1))
        y <- Invariants(t1, state1, pars, p, q, xpower)
        for (i in 1:n) {    # measurements in plot
            if (plotID == 23 && i == 1) next   # for plot 23, skip first measurement
            t2 <- d$age[i]
            state2 <- State(t2, y, pars, p, q, xpower)
            pred = rbind(pred, state2)
            if (interval && i < n) {
                state1["H"] <- d$H[i]
                state1["N"] <- d$N[i]
                state1["R"] <- as.vector(state2["R"])
                state1["B"] <- d$B[i]
                t1 <- t2
                y <- Invariants(t1, state1, pars, p, q, xpower)
            }
        } # end of plot
        out <- rbind(out, cbind(rbind(breastHt, d), pred))
     } # end of data
    names(out) <- c(names(data), "Hpred", "Npred", "R", "Bpred")
    return(out)
}

predint1 <- Predictions(pars1, spruceData, T, T)
# ... etc. ...
```

D Differential equations and System Dynamics implementation

The invariants approach provides explicit and computationally efficient solutions. It may be useful, however, to write down the model differential equations in the more traditional form. Their numerical integration serves as a check on the other implementations. We have a system of 4 differential equations, for the 4 state variables H, N. R, and B:

$$\frac{\mathrm{d}H}{\mathrm{d}t} = 46.1667 q^{1.29944} H^{0.4171} - 1.71556 q H \tag{39}$$

$$\frac{\mathrm{d}N}{\mathrm{d}H} = -4.57590 \times 10^{-15}\, H^{5.009} N^{2.9895} \tag{40}$$

$$\frac{\mathrm{d}R}{\mathrm{d}H} = 0.0234745 p H (1 - R) \tag{41}$$

$$\frac{\mathrm{d}B}{\mathrm{d}H} = 0.53449 p N^{0.3} [1 - (1 - R)^{2.2}] - B/H \\ - 1.37277 \times 10^{-15} H^{5.009} N^{1.9895} B \tag{42}$$

The last three equations can be expressed as derivatives with respect to t multiplying by the first one. Initial conditions at breast height are $H = 1.3$,

$N = N_{\mathrm{bh}}$, $R = 1.815103 \times 10^{-6}\, N_{\mathrm{bh}}$, $B = 0$. The q for site index 20 is 0.0202789.

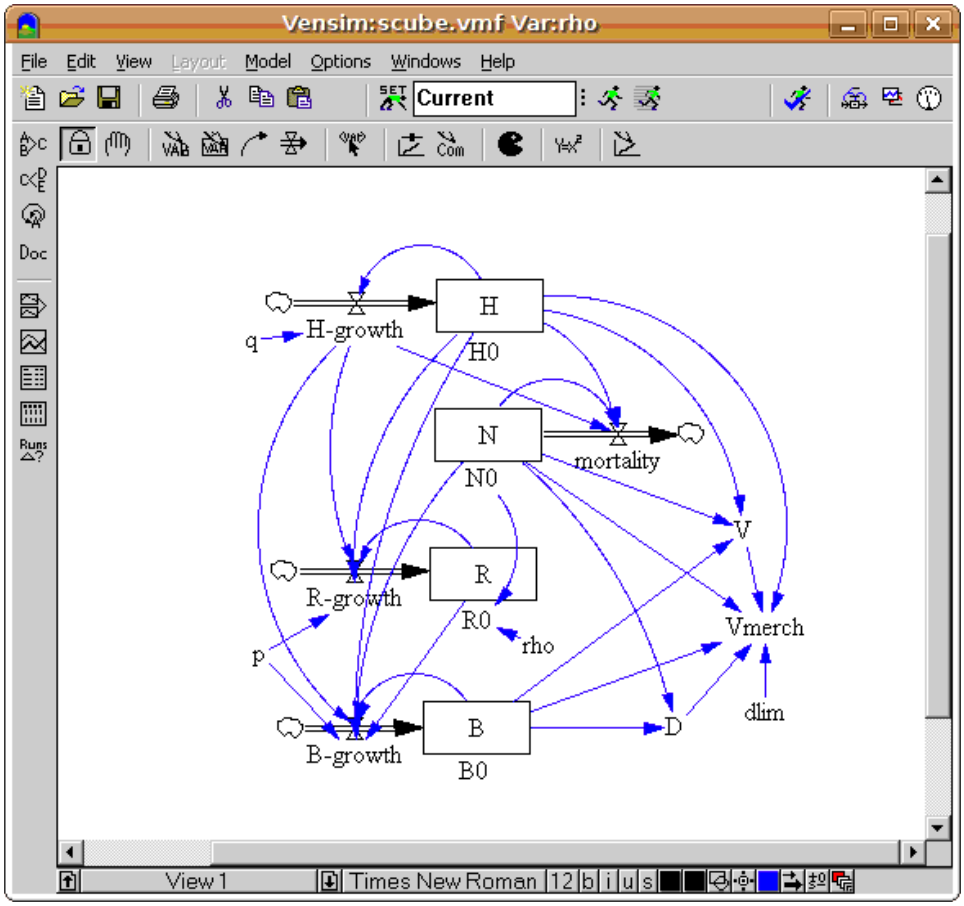

Figure 30: Implementation of (39)–(42) in Vensim.

Figure 30 shows a System Dynamics diagram in Vensim (`www.vensim.com/venple.html`). The 4th order Runge-Kutta numerical integration produced the same results as the R and Excel versions.